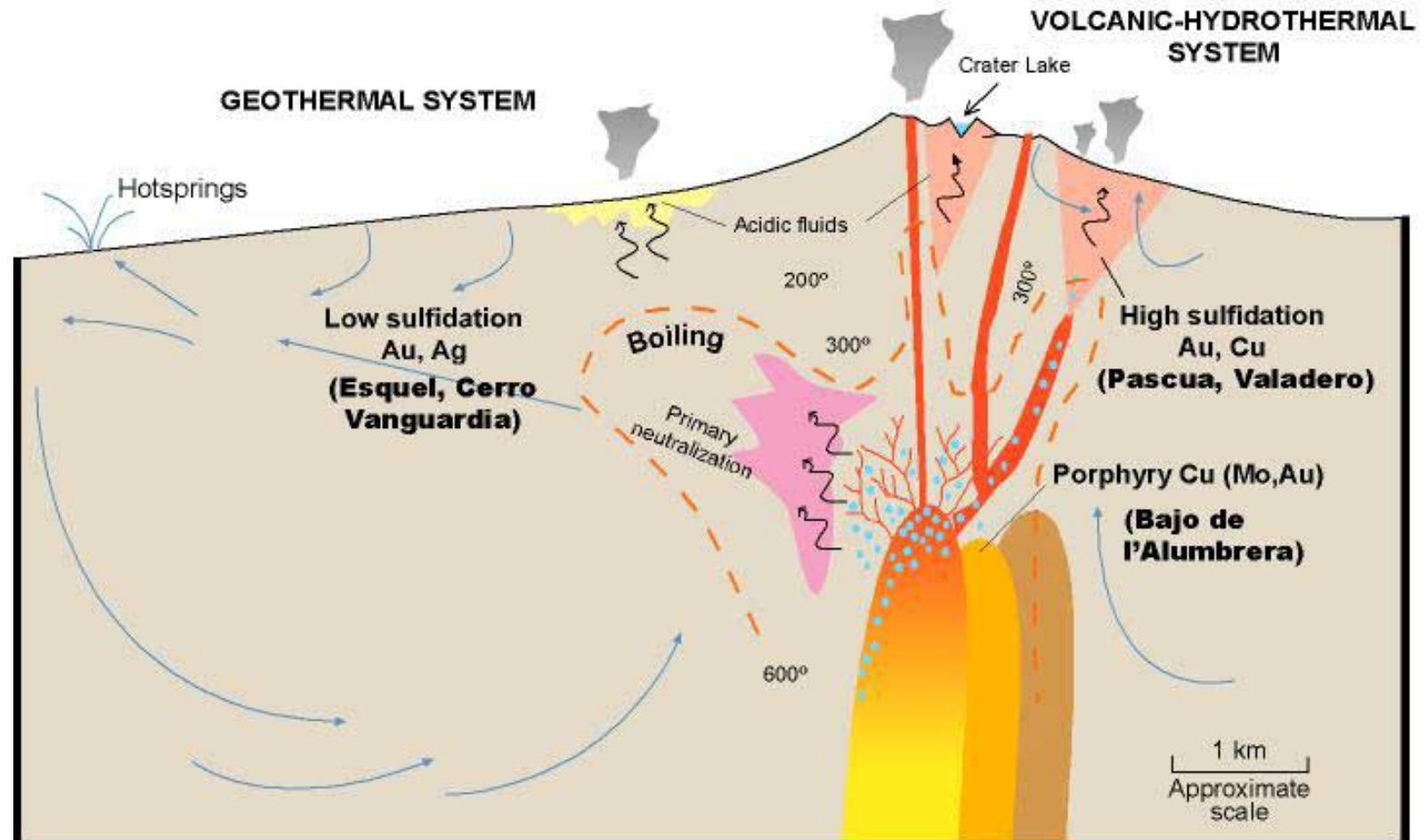


Epithermal Deposits

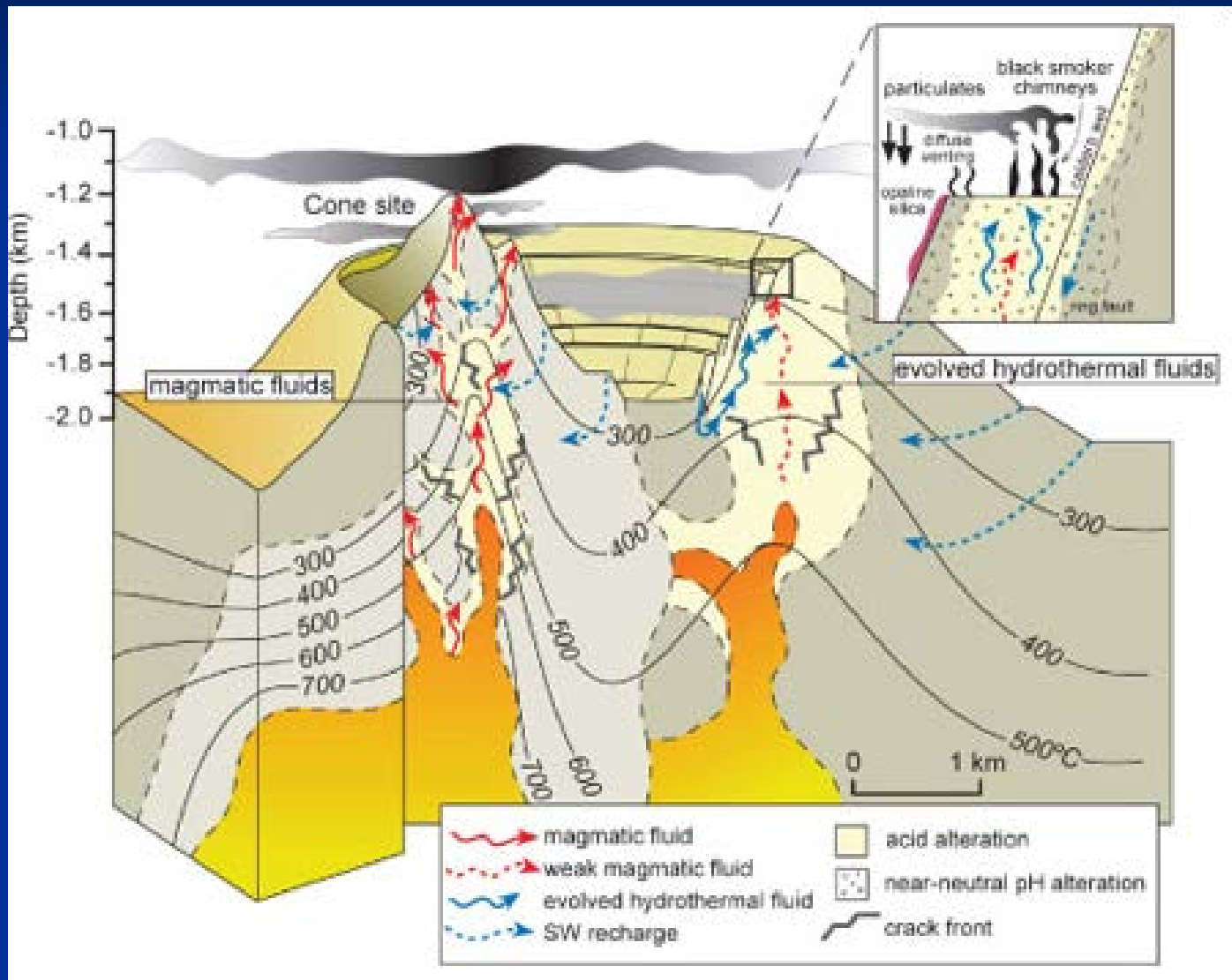
Epithermal Systems

Low and high sulphidation deposits

Schematic Cross-Section

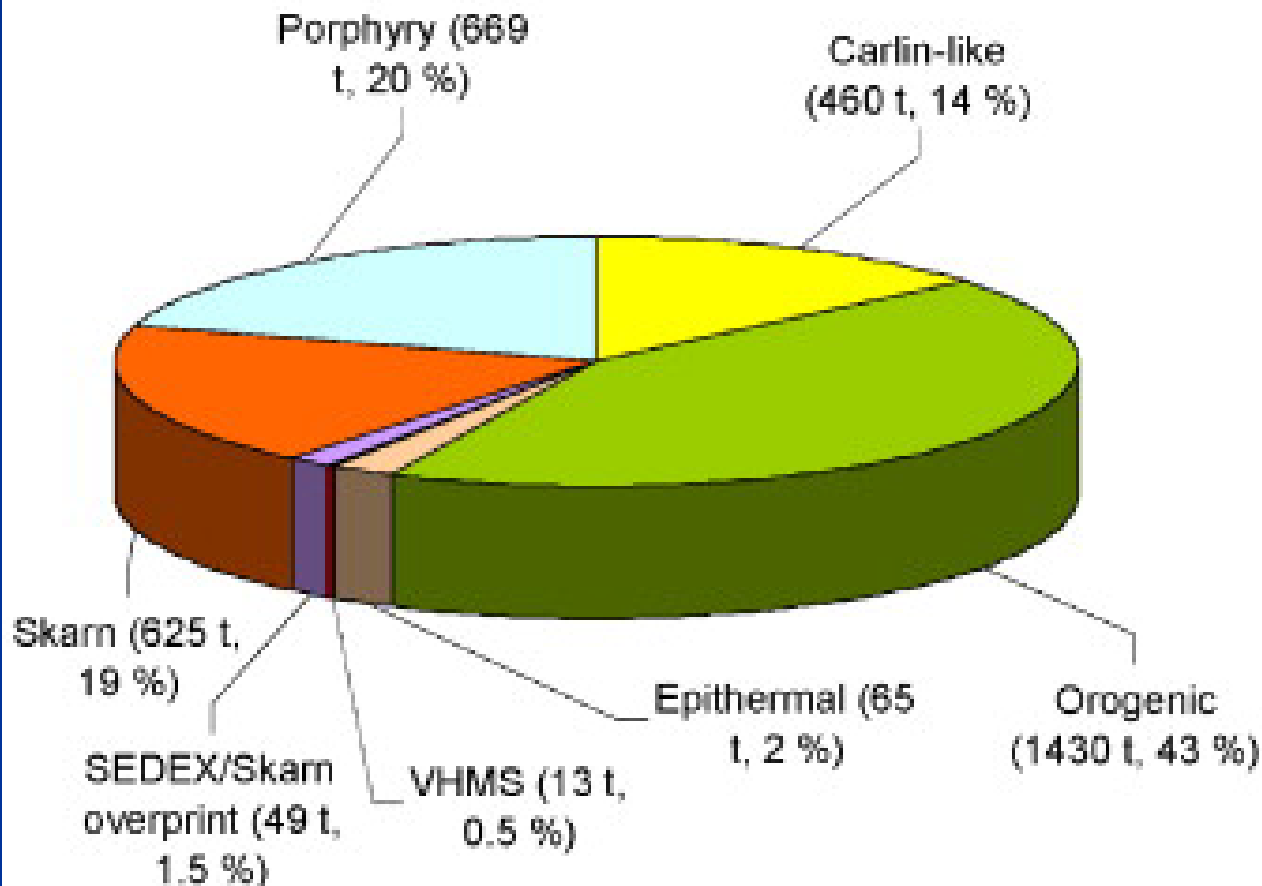


Submarine Epithermal Systems

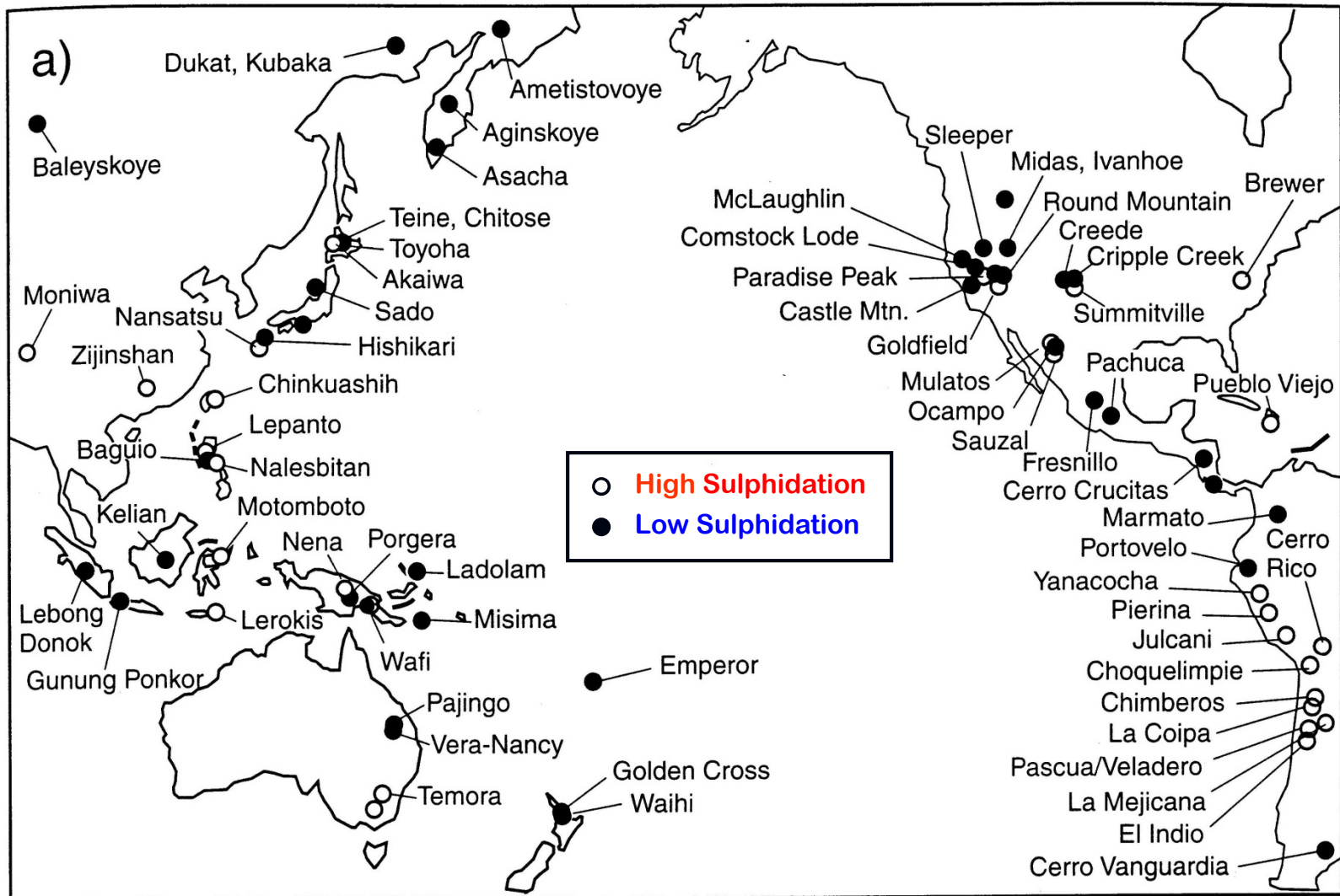


The significance of Epithermal Deposits as a Gold Resource

C. Gold resources



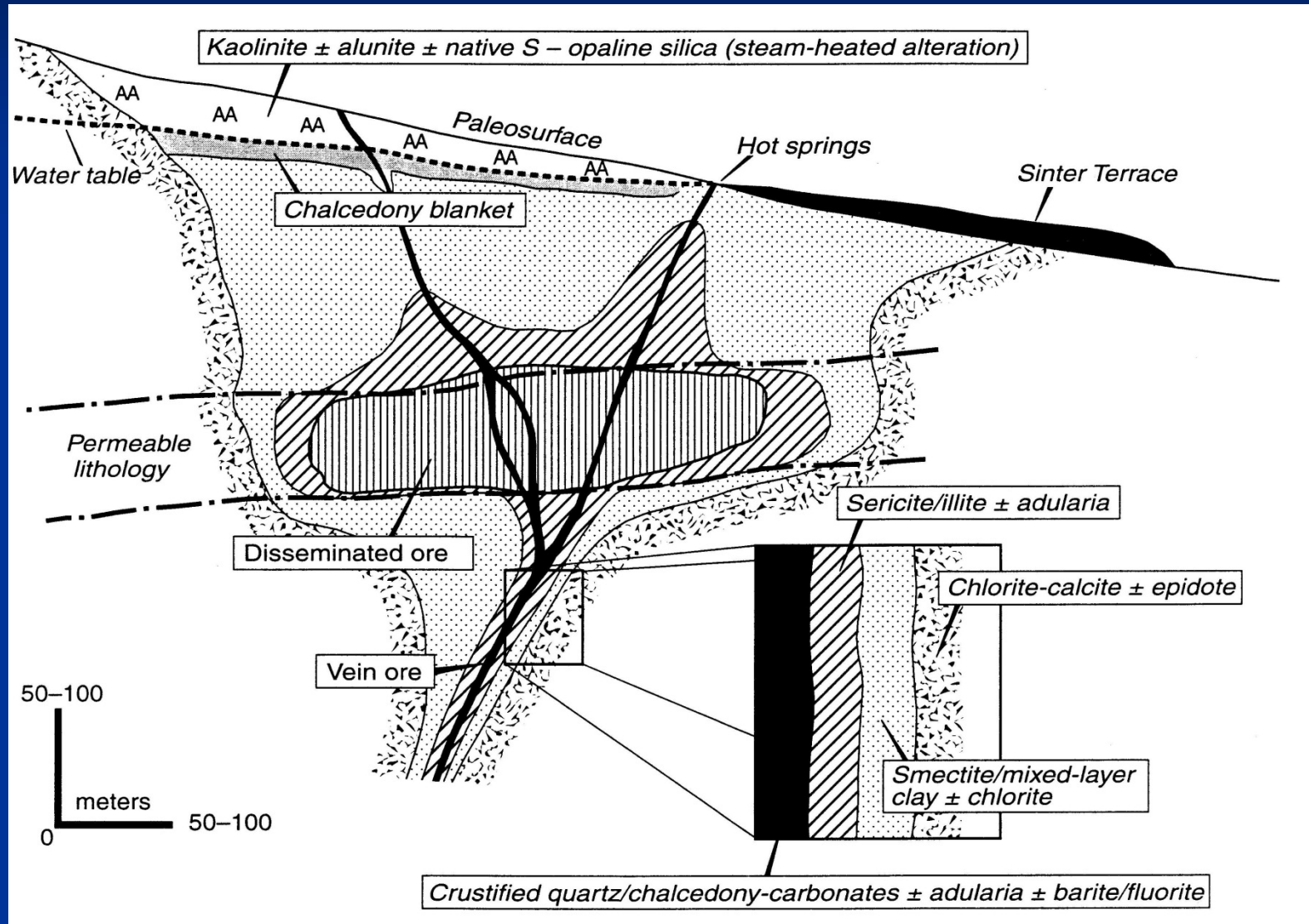
Distribution of Epithermal Deposits



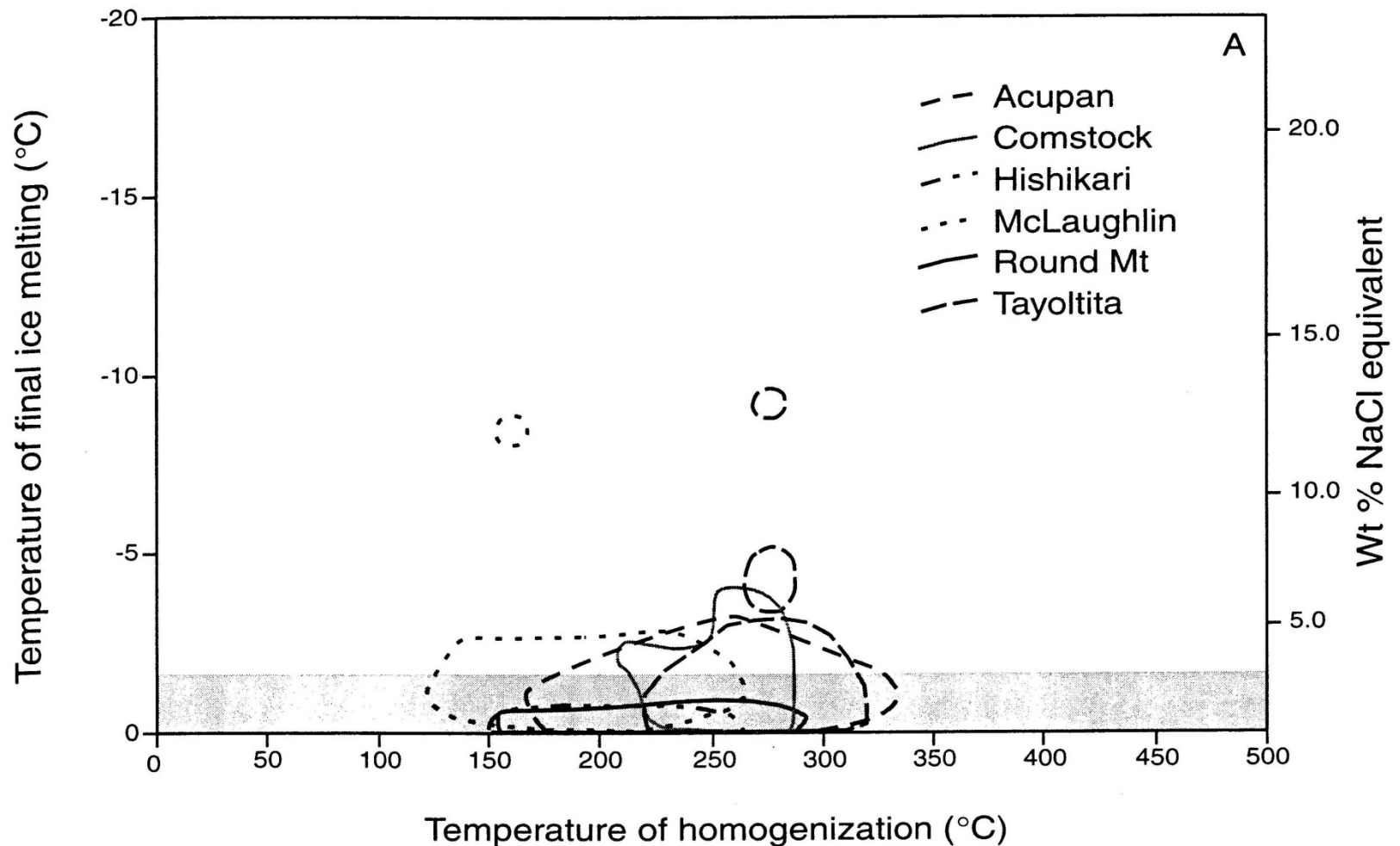
Surface expression of a low sulphidation epithermal deposit



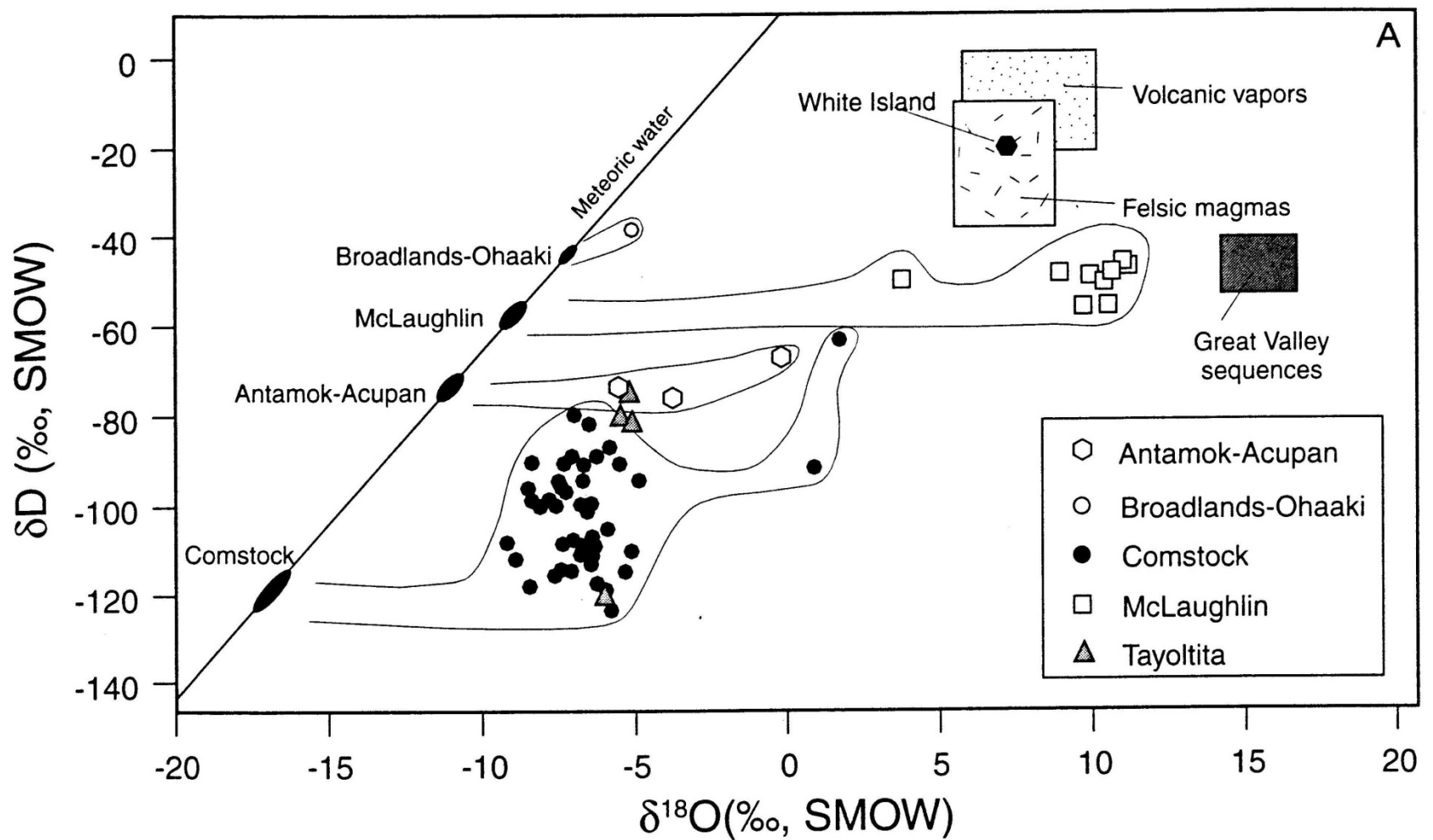
Low Sulphidation Deposits Ore Styles and Alteration Assemblages



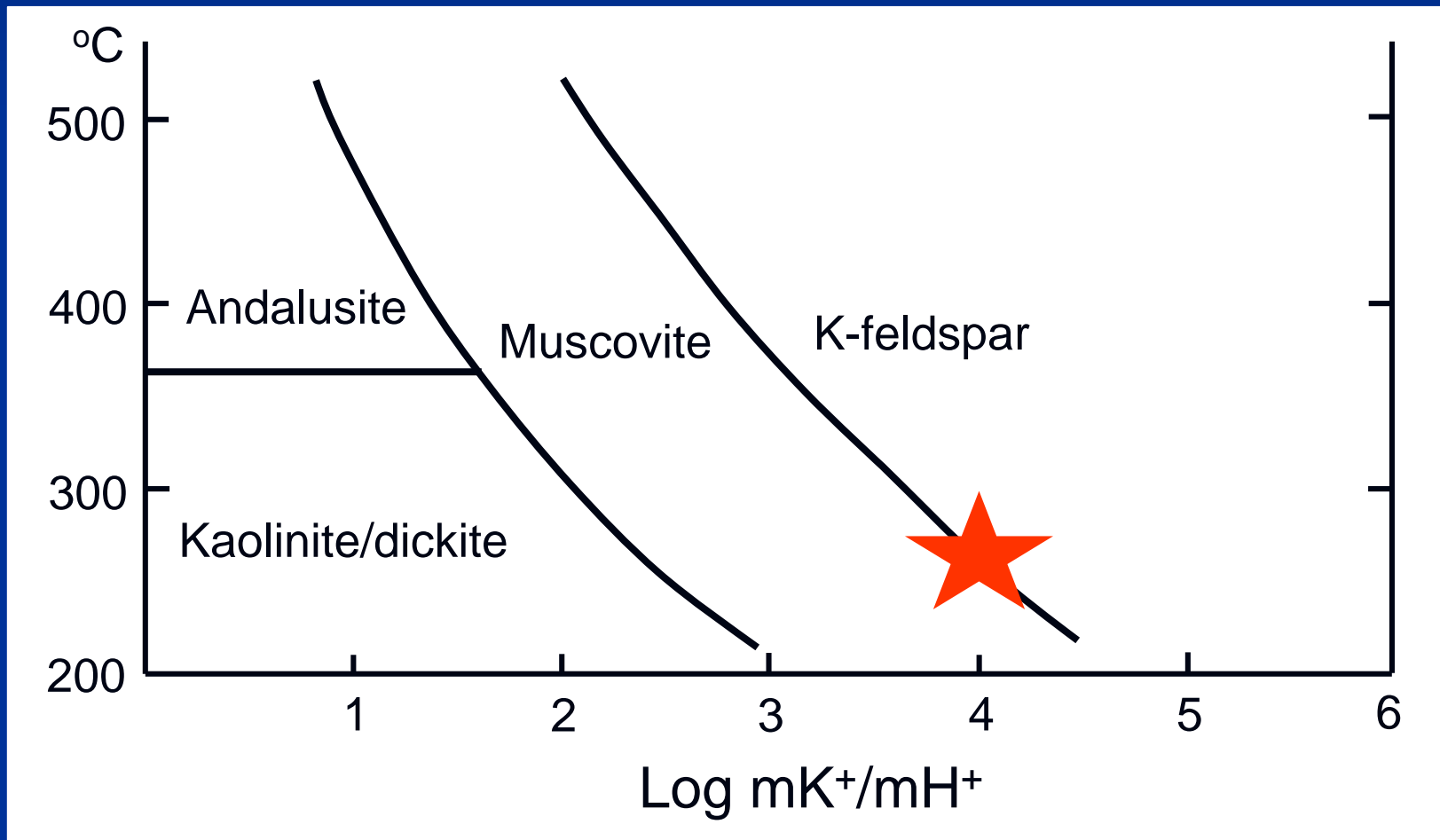
Low Sulphidation Deposits Fluid Inclusion Temperatures and Salinities



Low Sulphidation Deposits Oxygen and Hydrogen Isotopic Data



Low Sulphidation Deposits Temperature-pH Conditions



The Low Sulphidation Epithermal – Geothermal Link

Champagne Pool, New Zealand



Up to 90 g/t Au

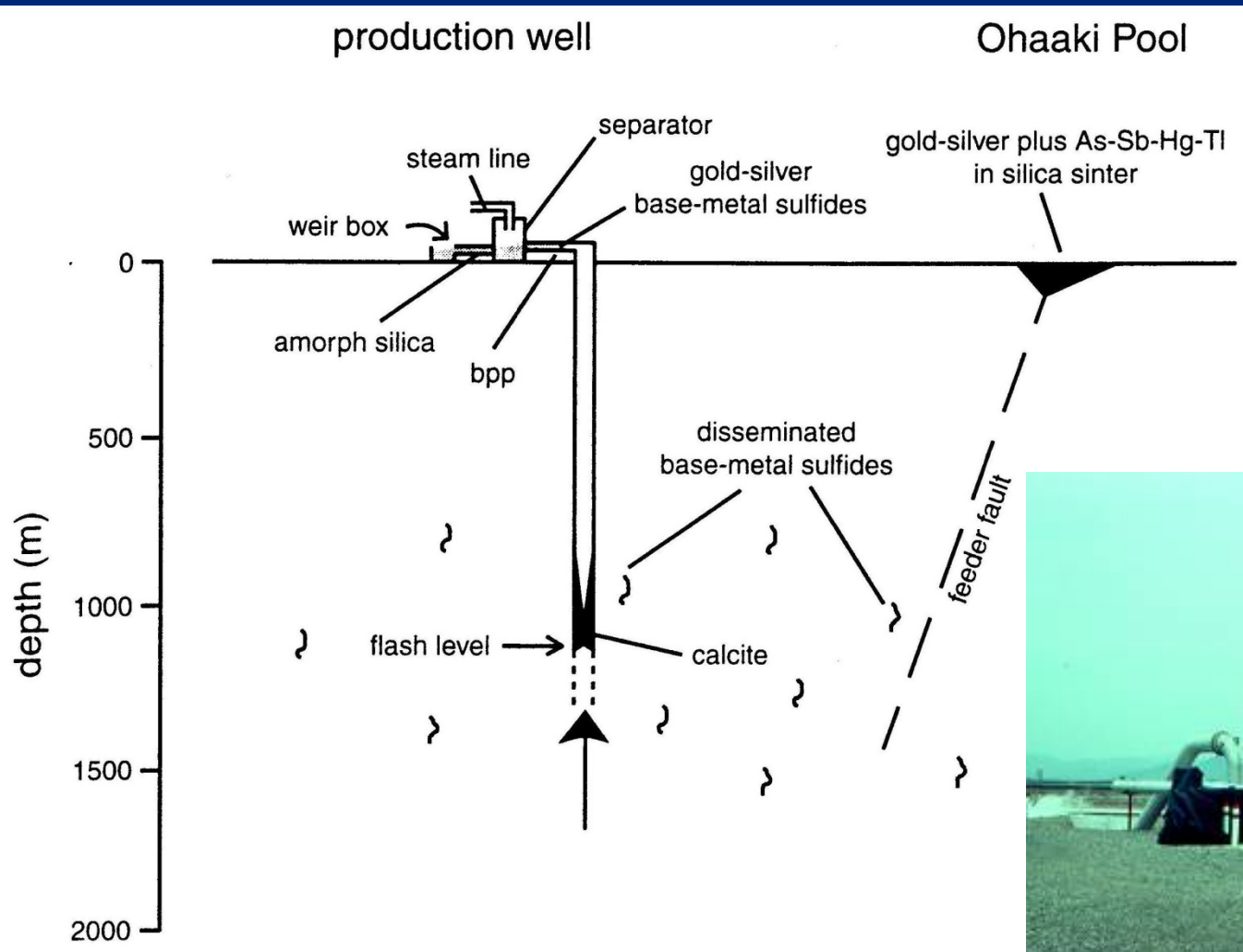
Old Faithful, Yellowstone



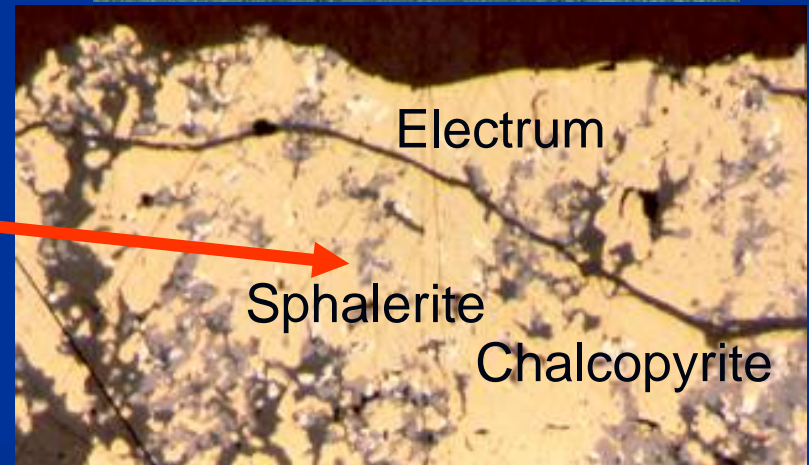
Wairakei Geothermal Power Plant, New Zealand



The Low Sulphidation Epithermal – Geothermal Link

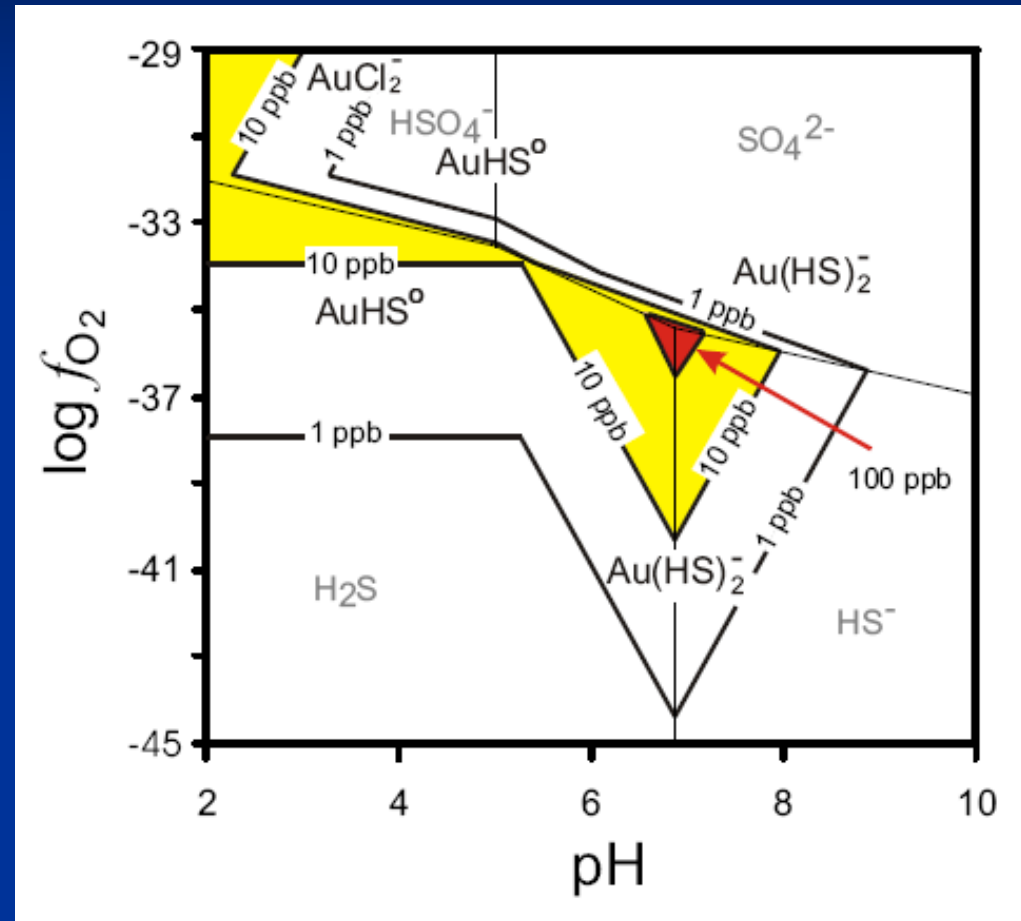
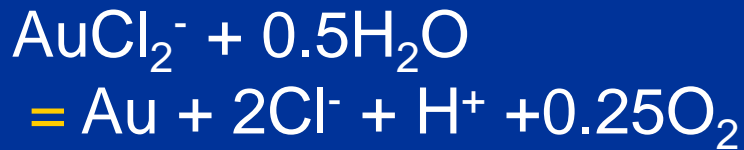
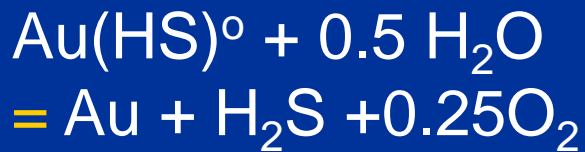
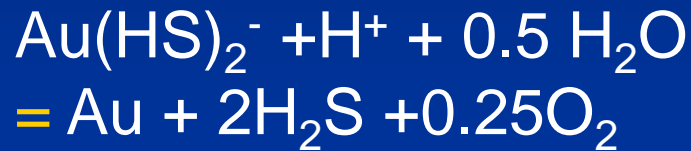


Geothermal Well Scalings from Cerro Prieto, Mexico

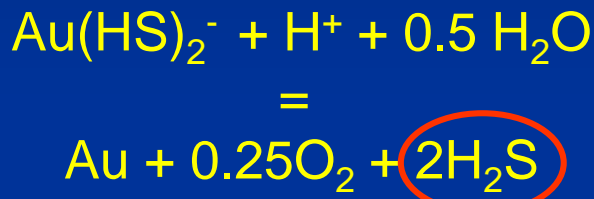


Clark, J.R. & Williams-Jones, A.E., (1990) Analogues of epithermal gold-silver deposition in geothermal well scales: *Nature*, v. 346, no. 6285, pp 644-645.

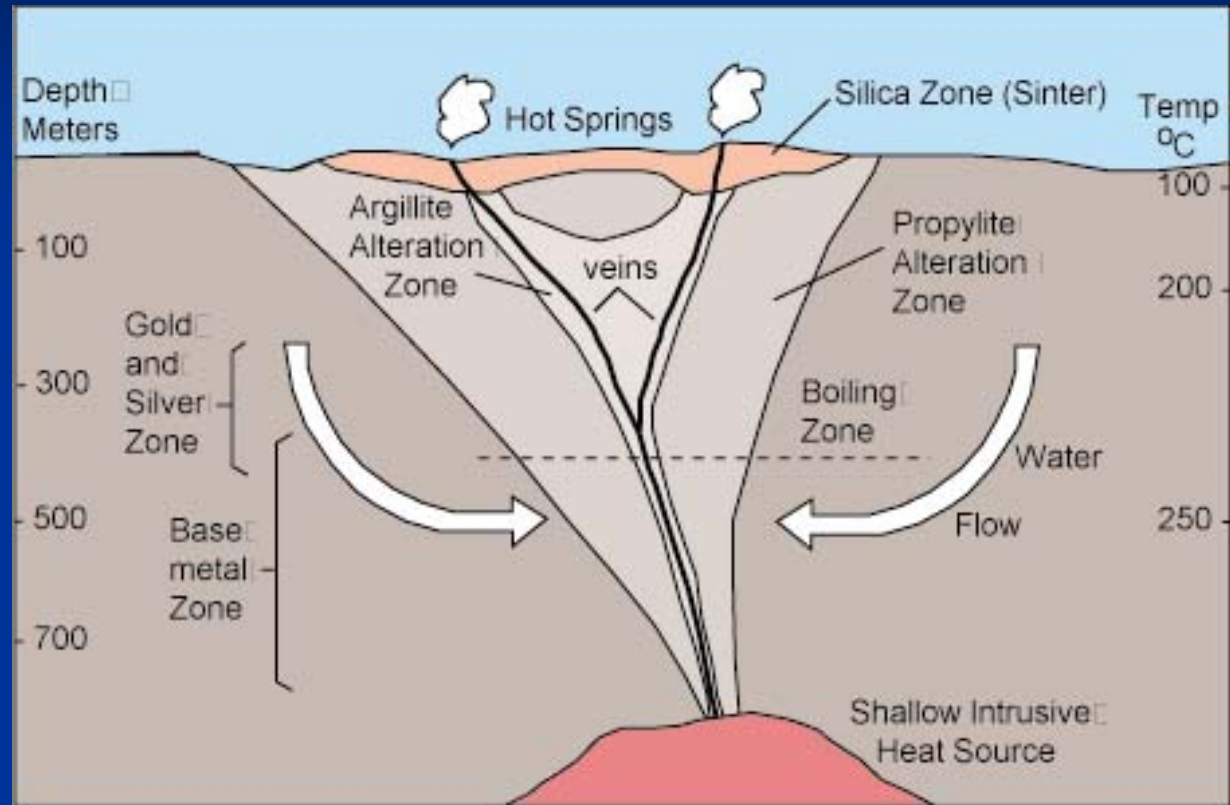
Controls on the Solubility of Gold



A model for the formation of low sulphidation epithermal deposits



Removed by boiling

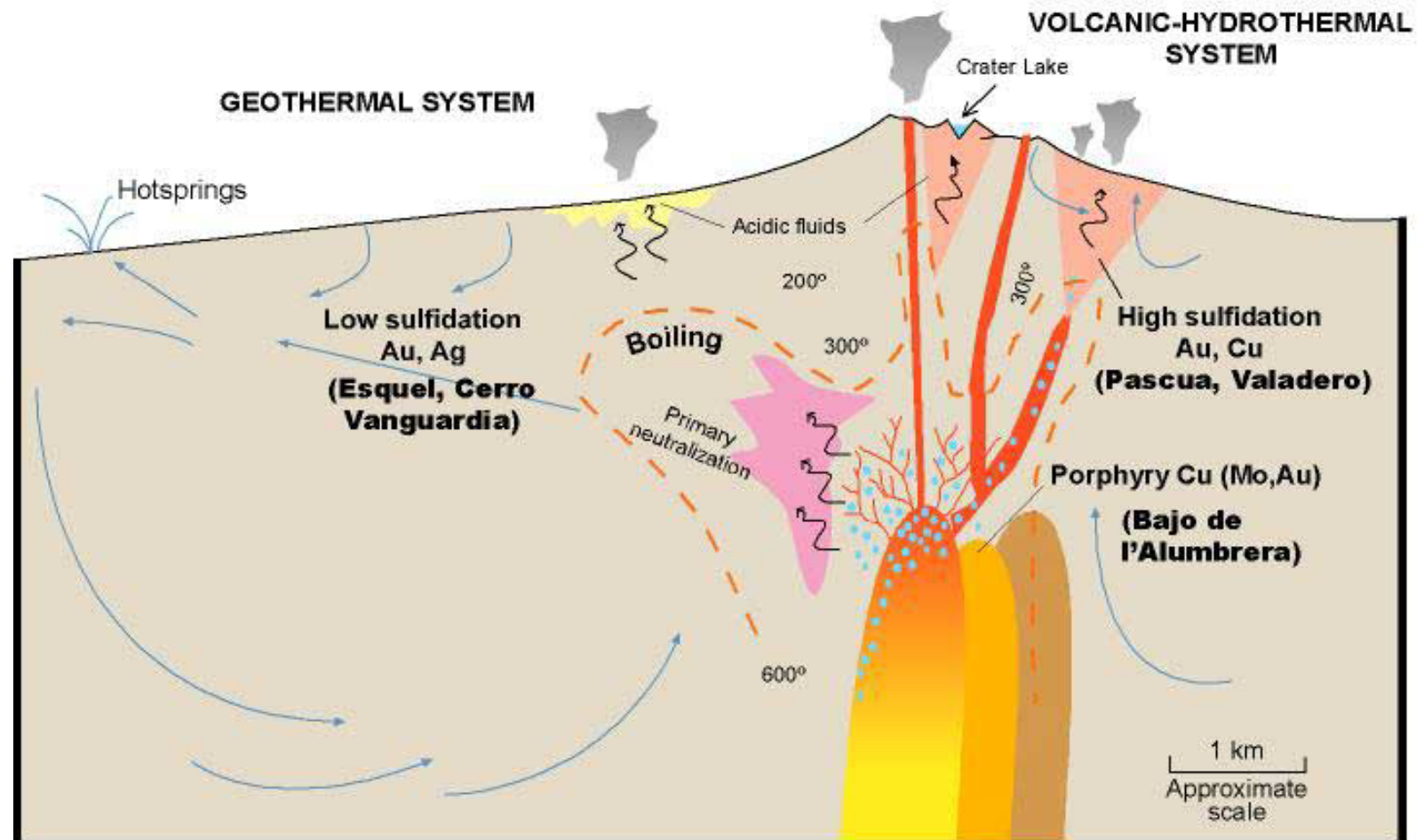


- 1) Magmatic vapour condenses in meteoric water
- 2) Gold transported as $\text{Au}(\text{HS})_2^-$
- 3) Water rises and boils, releasing H_2S and destabilizing $\text{Au}(\text{HS})_2^-$
- 4) Gold deposits as the native metal

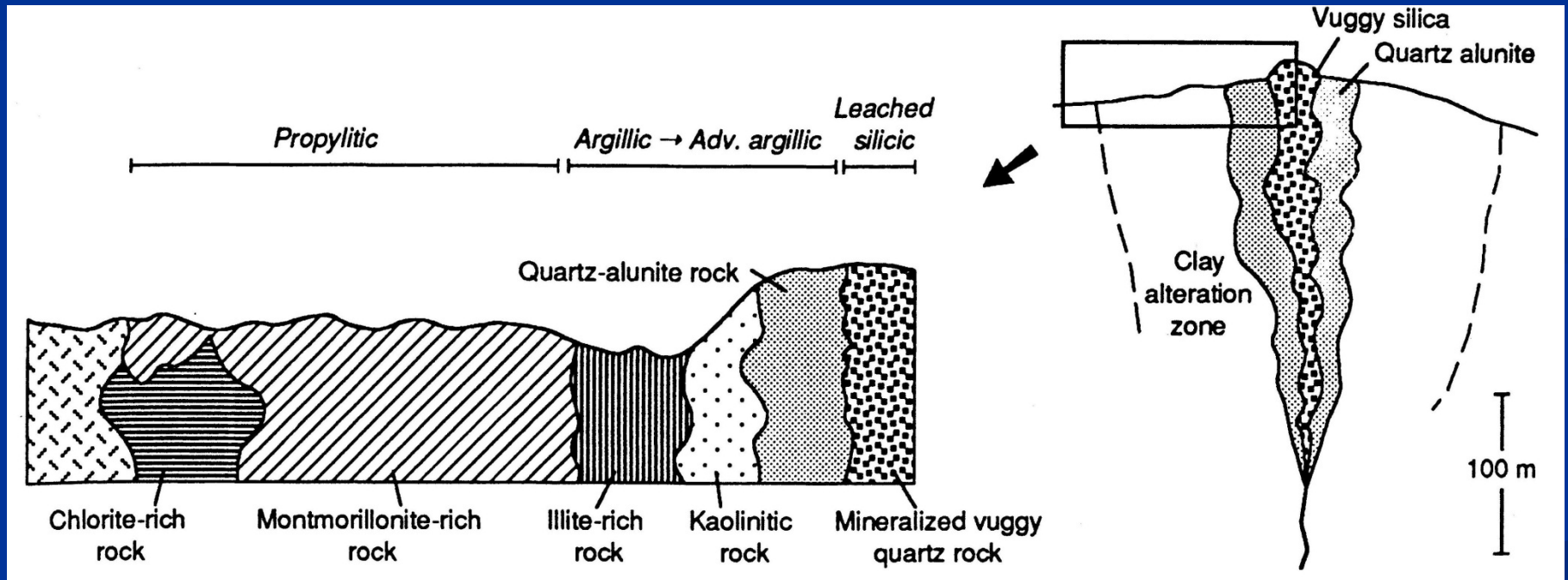
Epithermal Systems

High sulphidation deposits

Schematic Cross-Section



High Sulphidation Deposits Ore Style and Alteration Assemblages



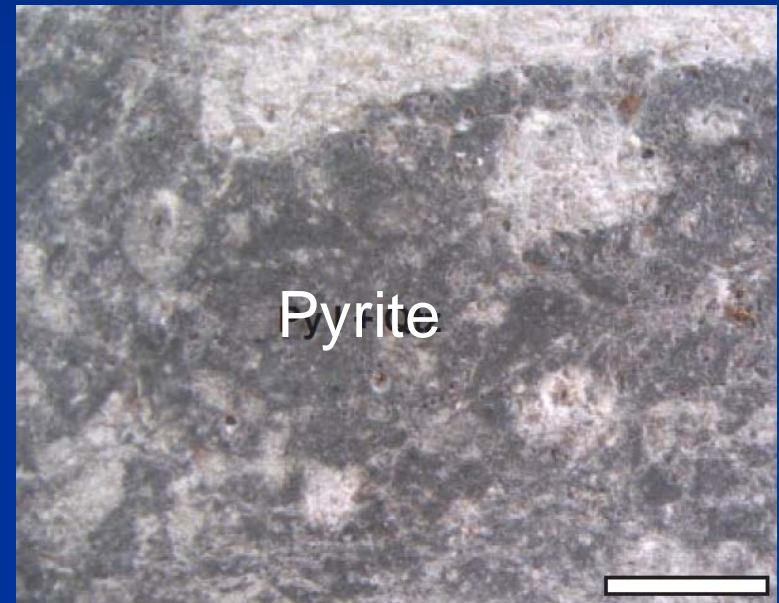
Acid-Sulphate Alteration

Vuggy silica



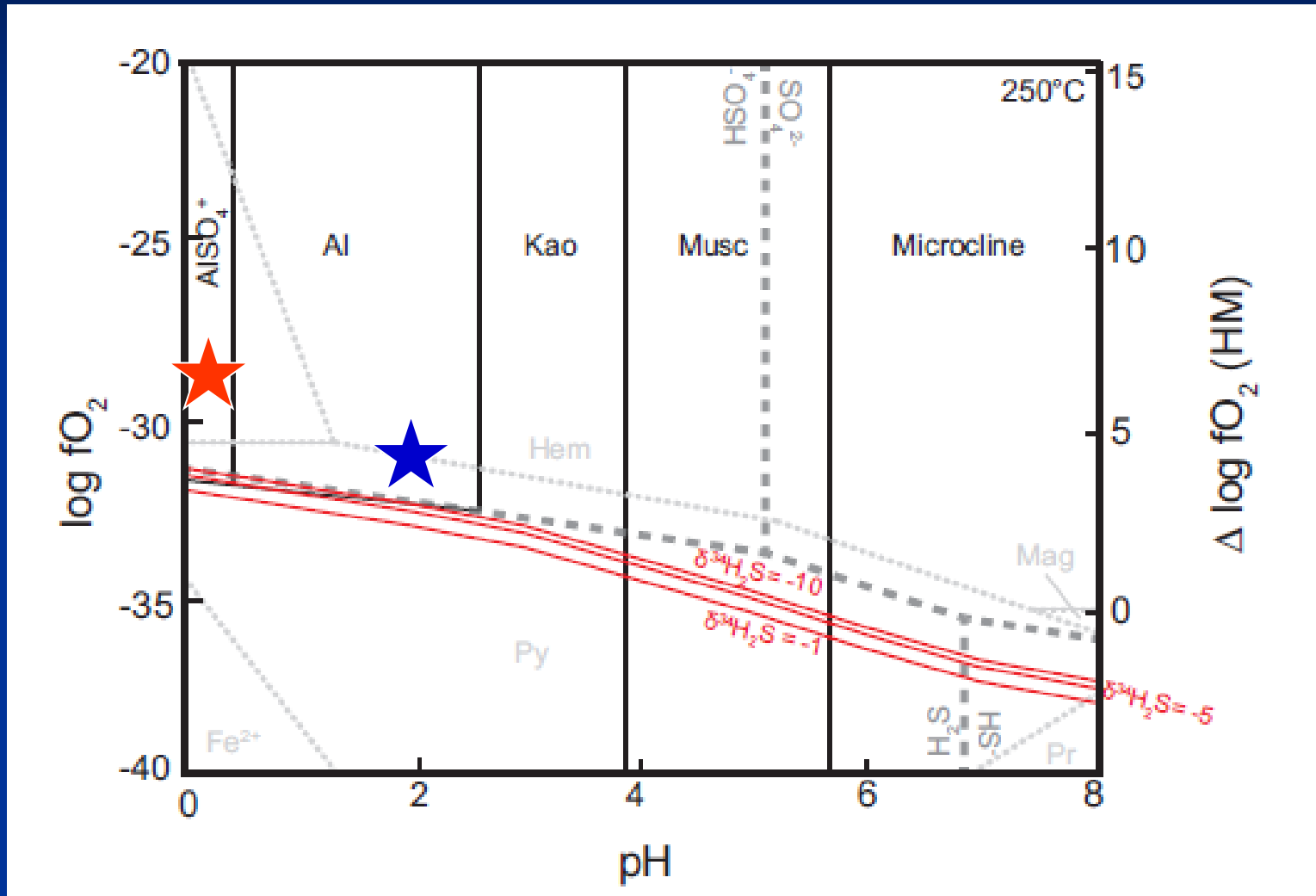
All components of the rock leached leaving behind vuggy silica (pH < 1)

Advanced argillic alteration

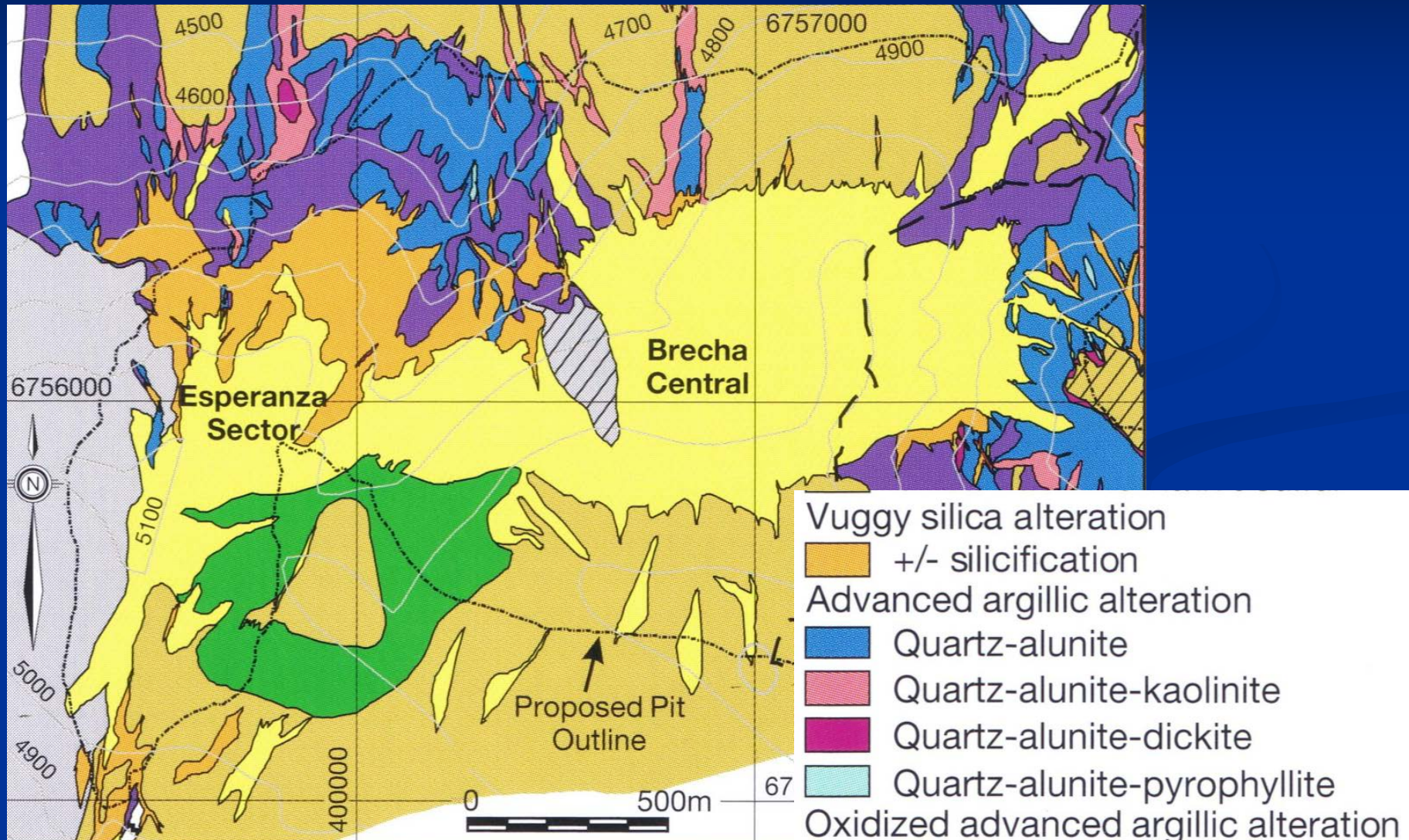


Alunite ($\text{KAl}_3(\text{SO}_4)_2(\text{OH})_6$)
Kaolinite ($\text{Al}_2\text{Si}_2\text{O}_5(\text{OH})_4$)
Quartz and Pyrite

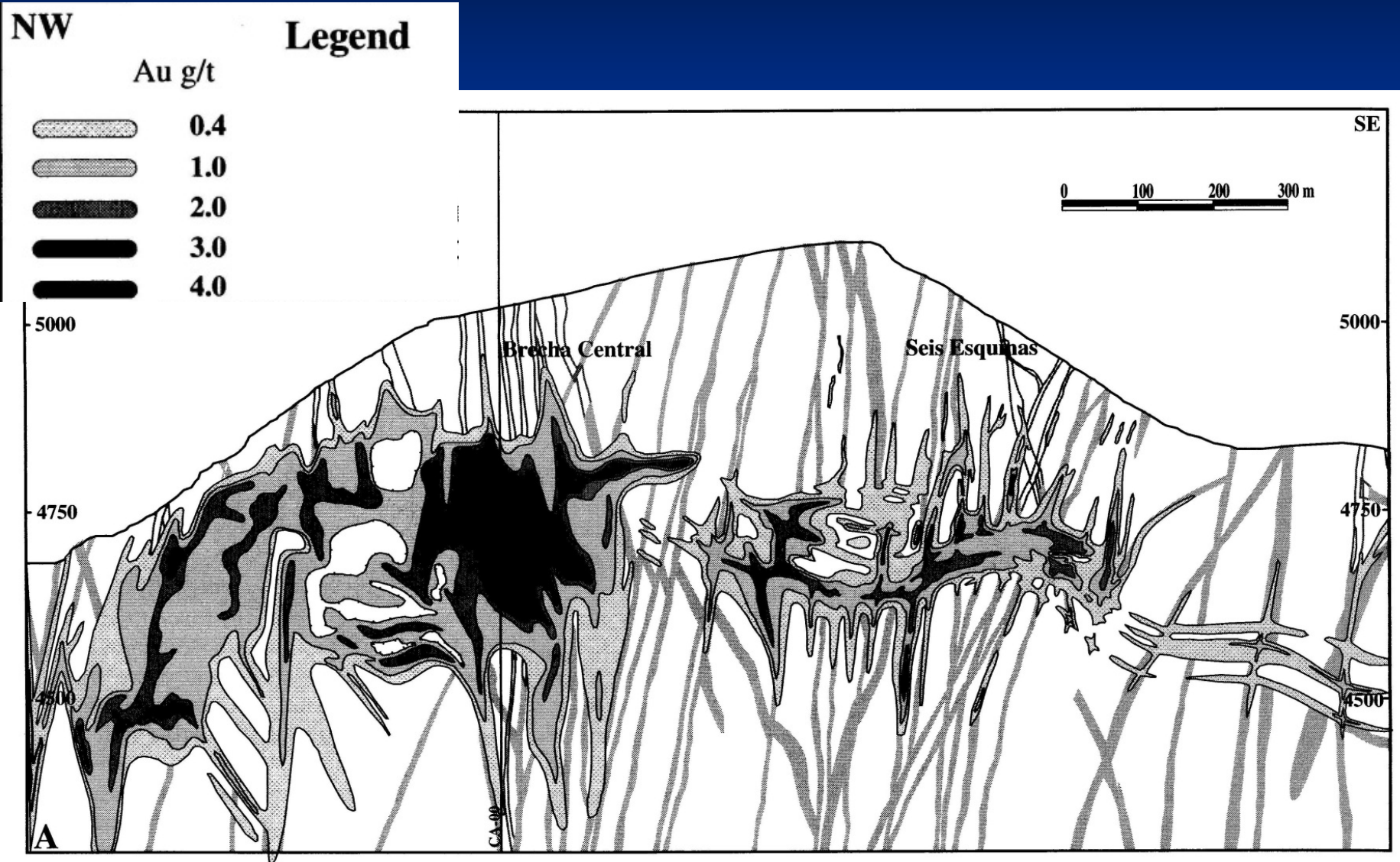
Conditions of Acid-Sulphate Alteration



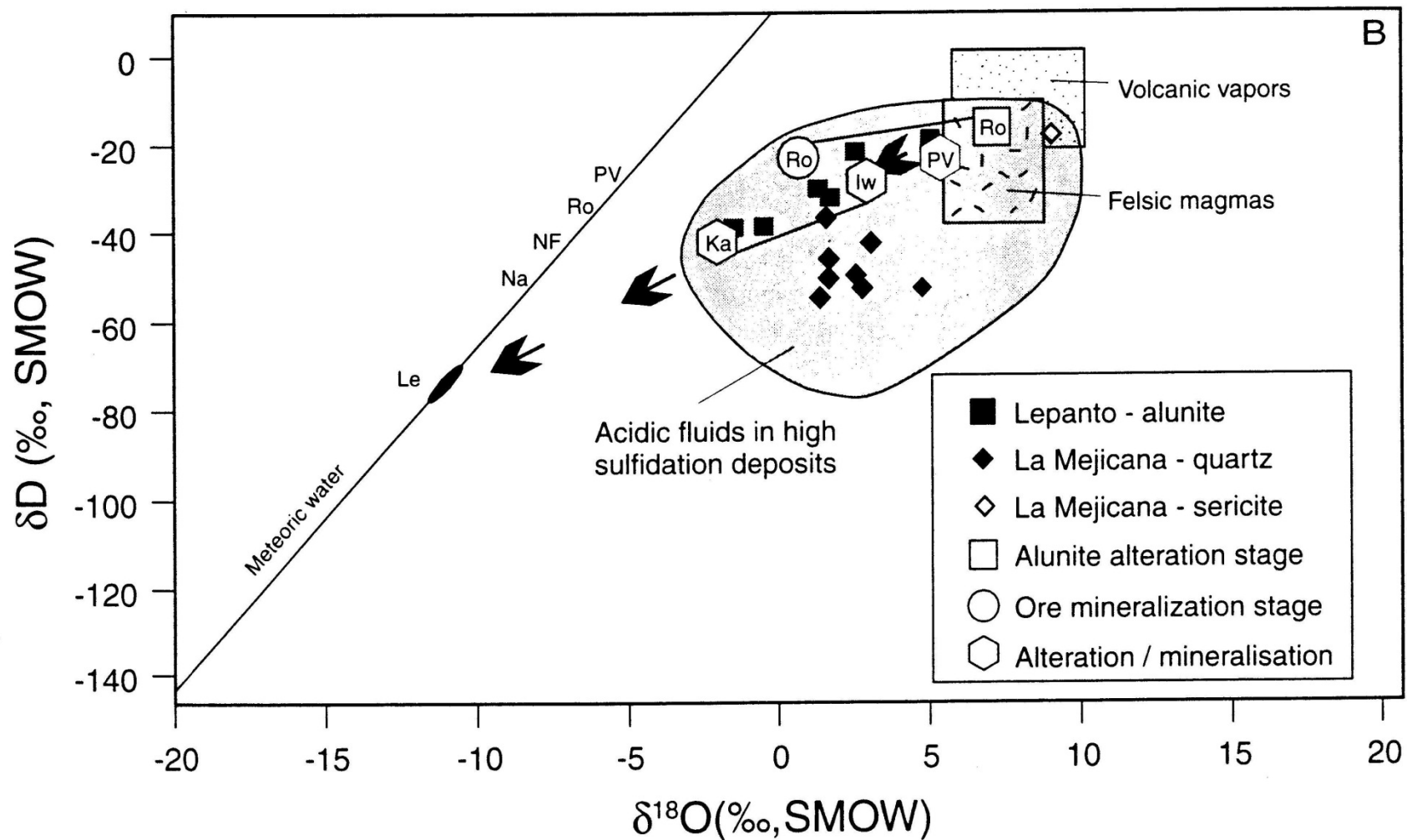
The high sulphidation Pascua epithermal deposit, Chile



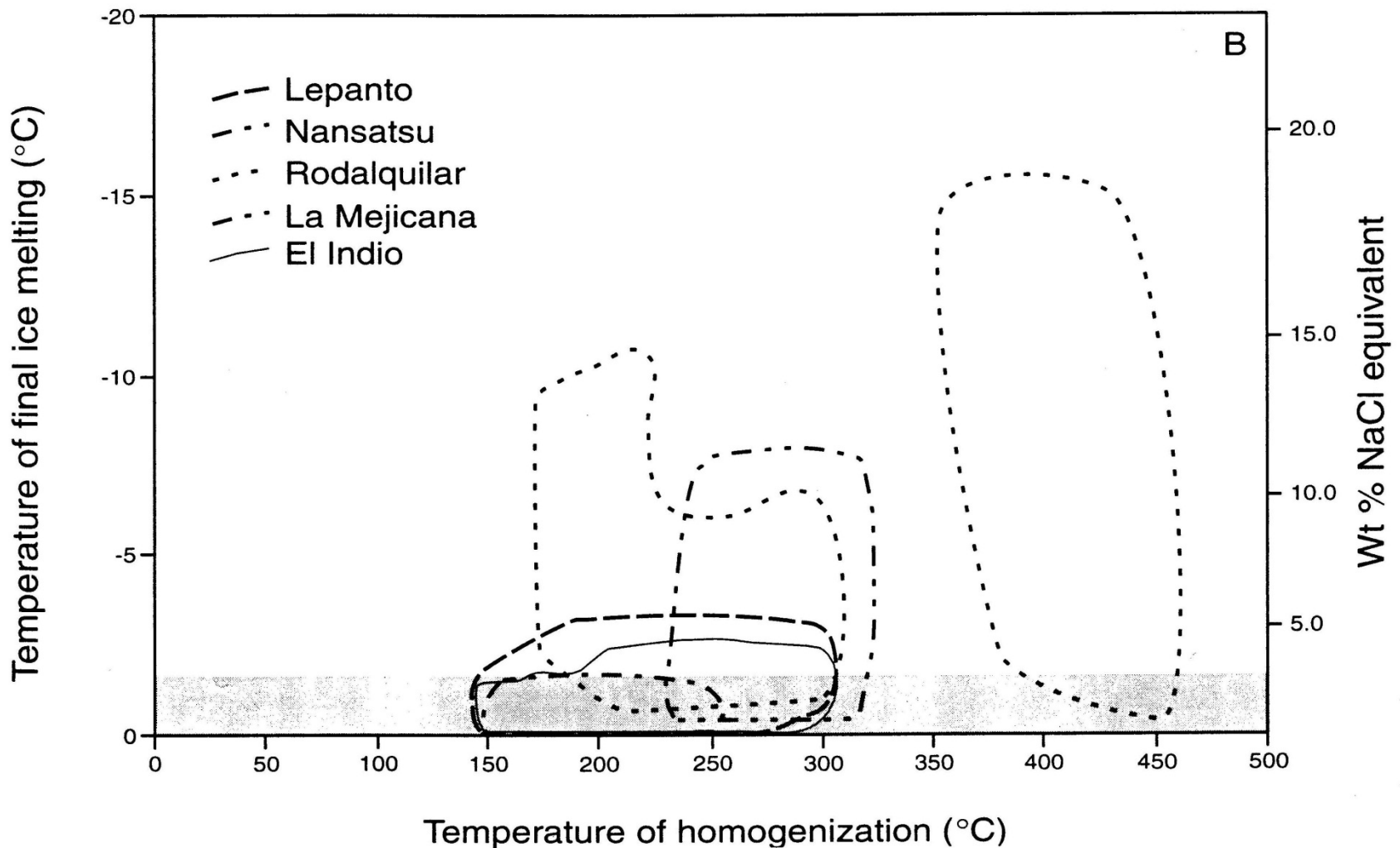
Mineralization at Pascua



High Sulphidation Deposits Oxygen and Hydrogen Isotopic Data



High Sulphidation Deposits Fluid Inclusion Temperatures and Salinities



A Model for the Formation of High Sulphidation Deposits

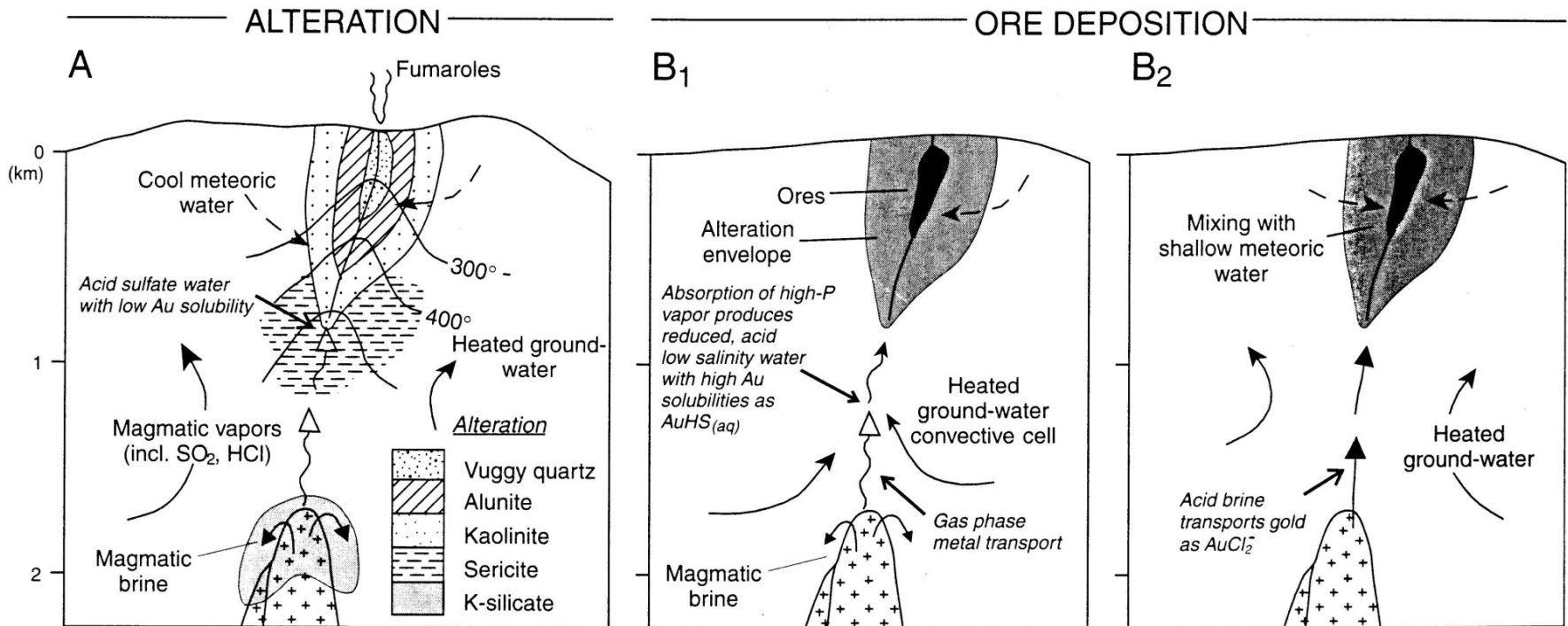
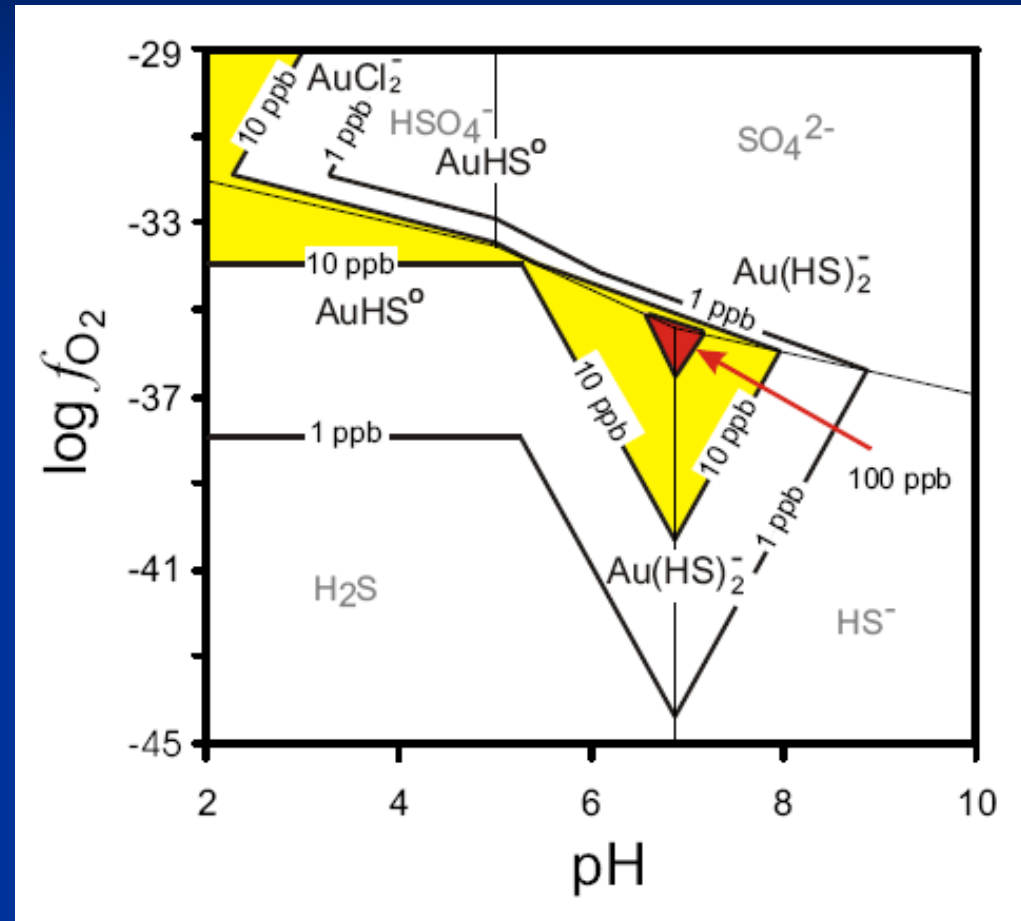
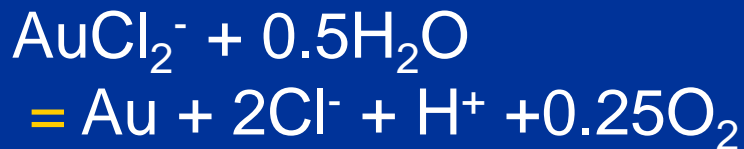
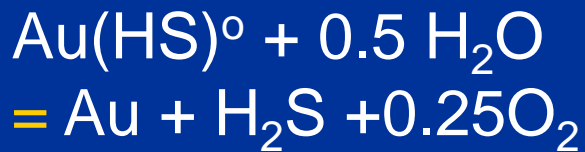
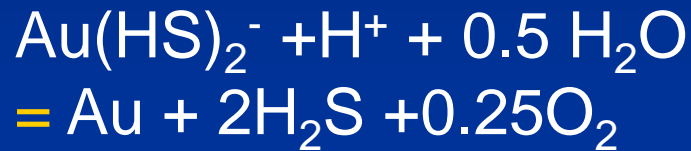
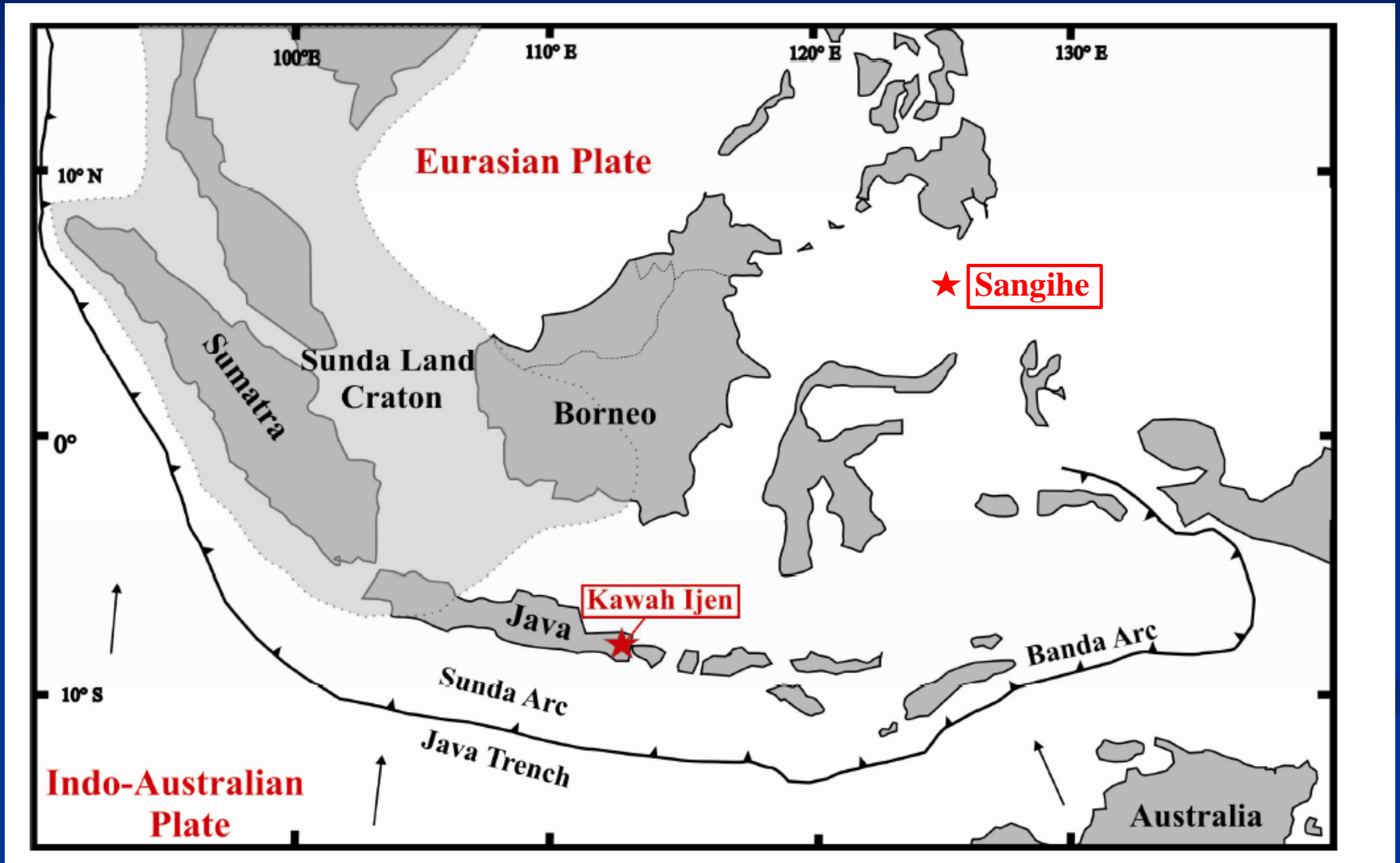


FIG. 12. Two-stage model for high-sulphidation ore formation proposed by Arribas (1995), modified to highlight likely water compositions involved in each stage of ore genesis. Stage 1 (A) is the ground preparation stage, whereby magmatic gases generate an acid sulfate high-sulphidation water that is responsible for the initial barren stage of residual silica and advanced argillic alteration. The second stage involves gold deposition from acid chloride low-sulphidation waters (B₁) or acid chloride brines (B₂).

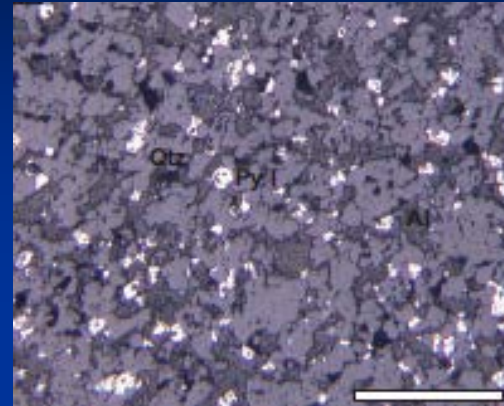
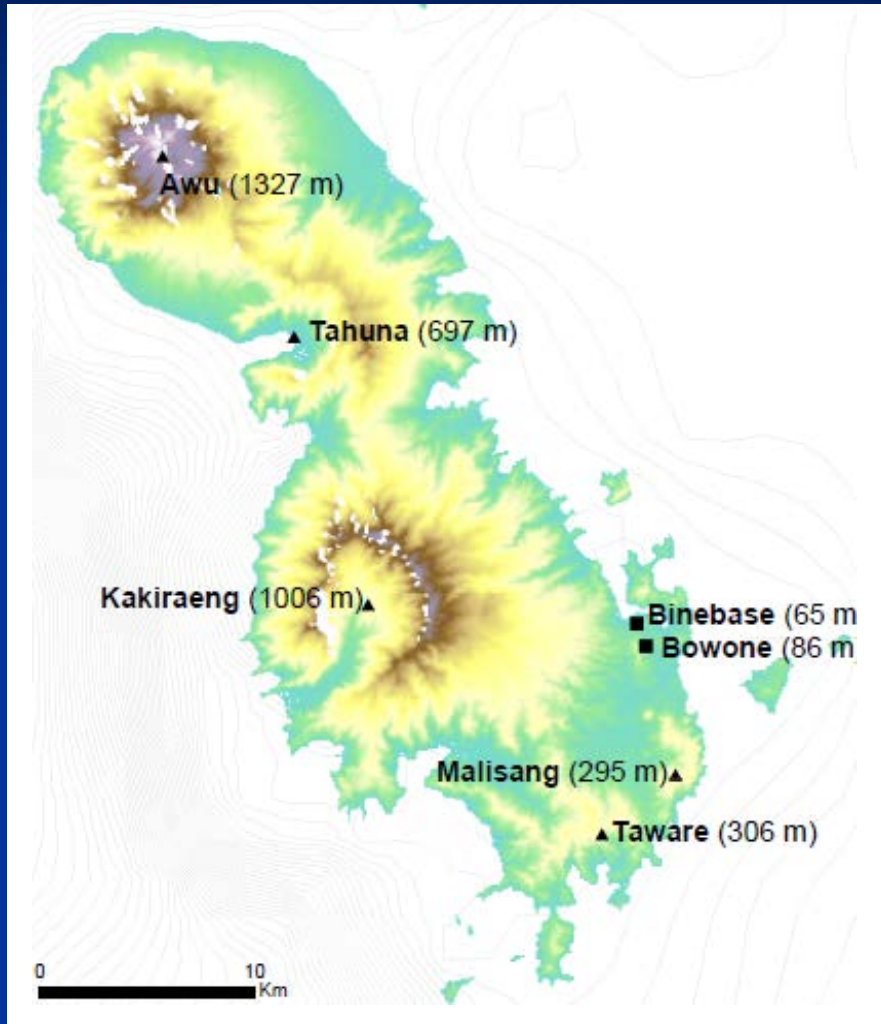
Controls on the Solubility of Gold



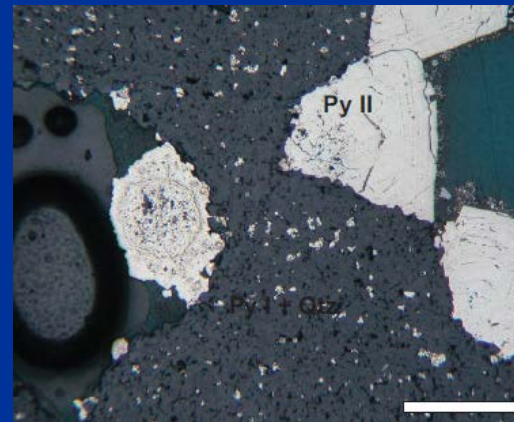
Lessons from Indonesia



The Sangihe Au-Ag Deposits



Py I Au 1.1 ppm
Ag 33 ppm

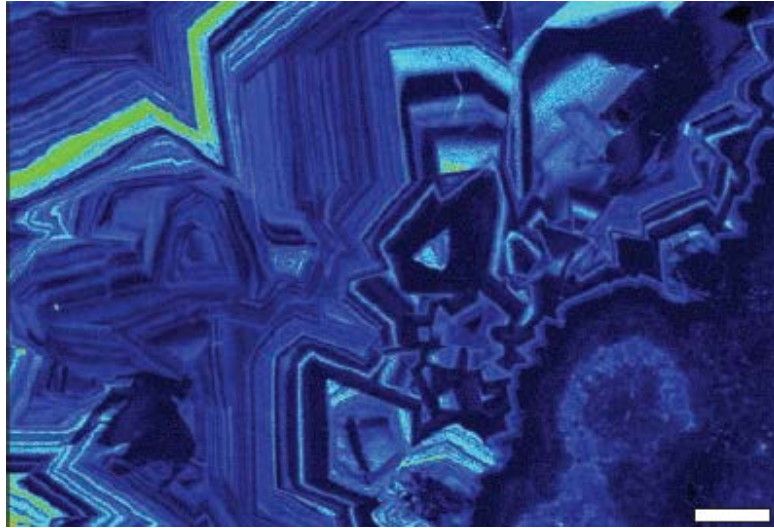


Py II Au 1 ppm
Ag 81 ppm

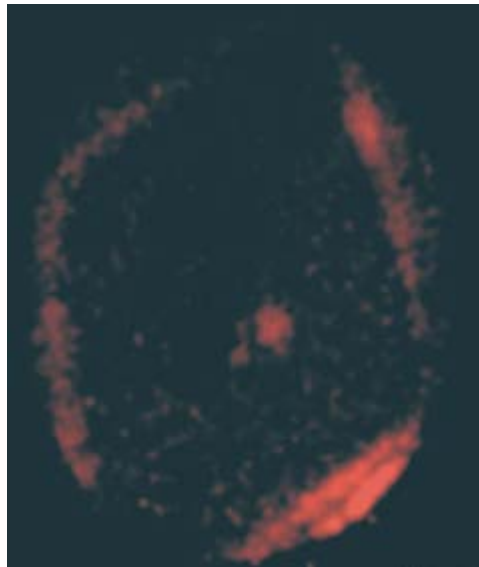
Deposit		tonnes (t)	Au (g/t)	Ag (g/t)
Bawone	Sulphide	5,999,000	1.12	0.97
Binebase	Oxide	7,851,000	1.10	25.13
	Sulphide	10,002,000	0.49	13.60

Metal zoning in pyrite

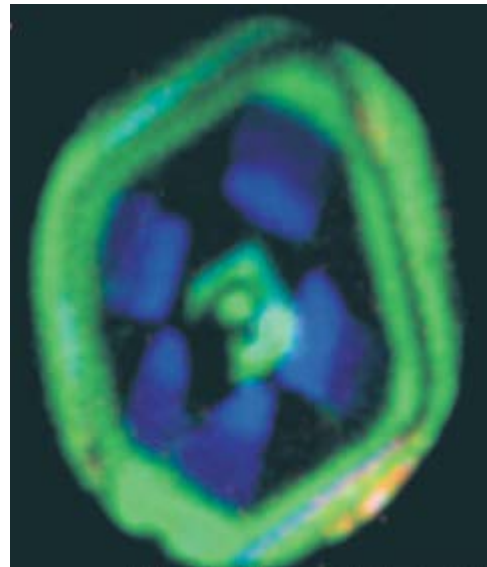
Copper map for
Py II at Sangihe



Gold map for
pyrite at
Pascua



Cu (green) As
(blue) maps for
pyrite at Pascua



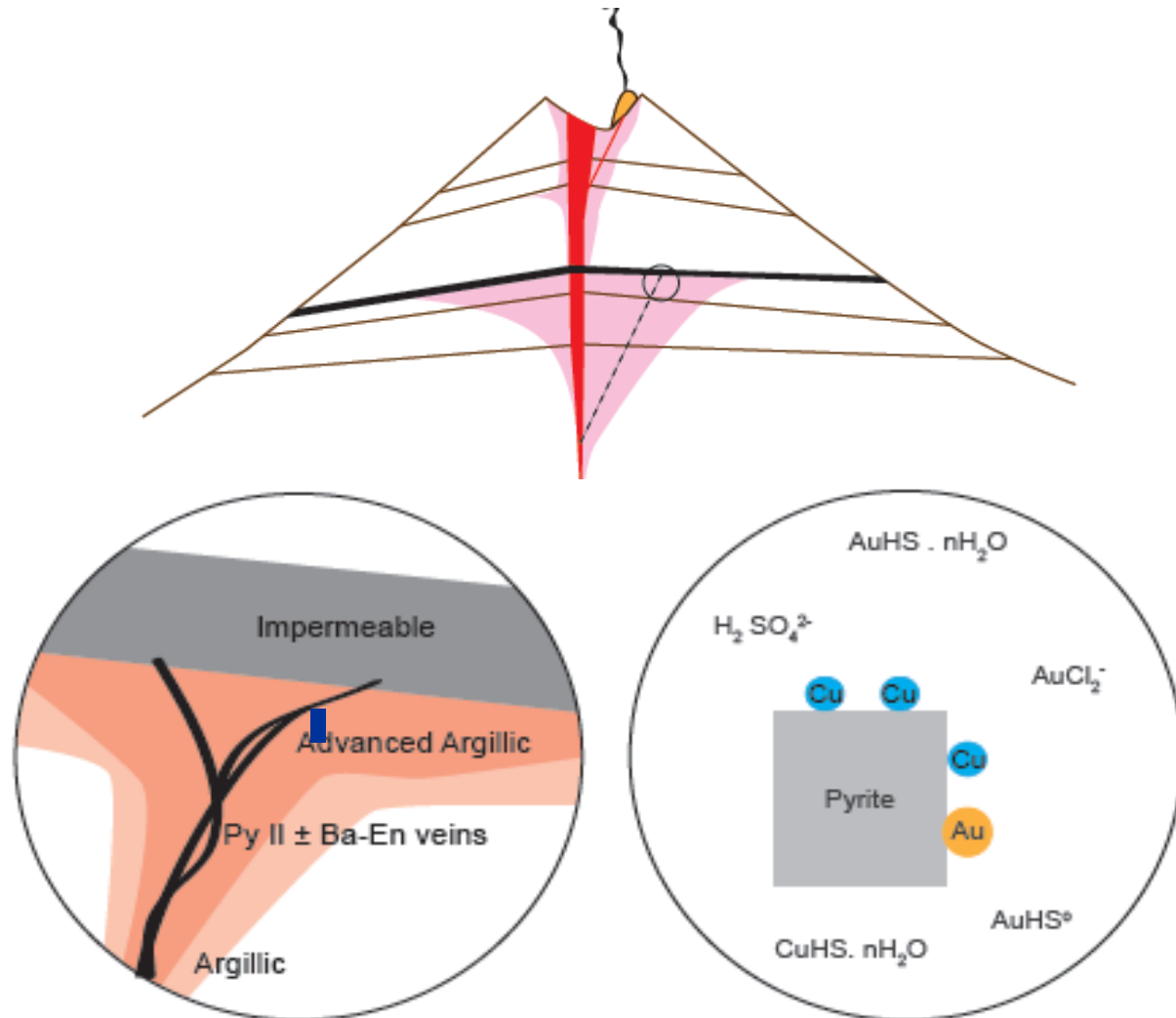
The Lycurgus Cup – dichroic glass and nanogold



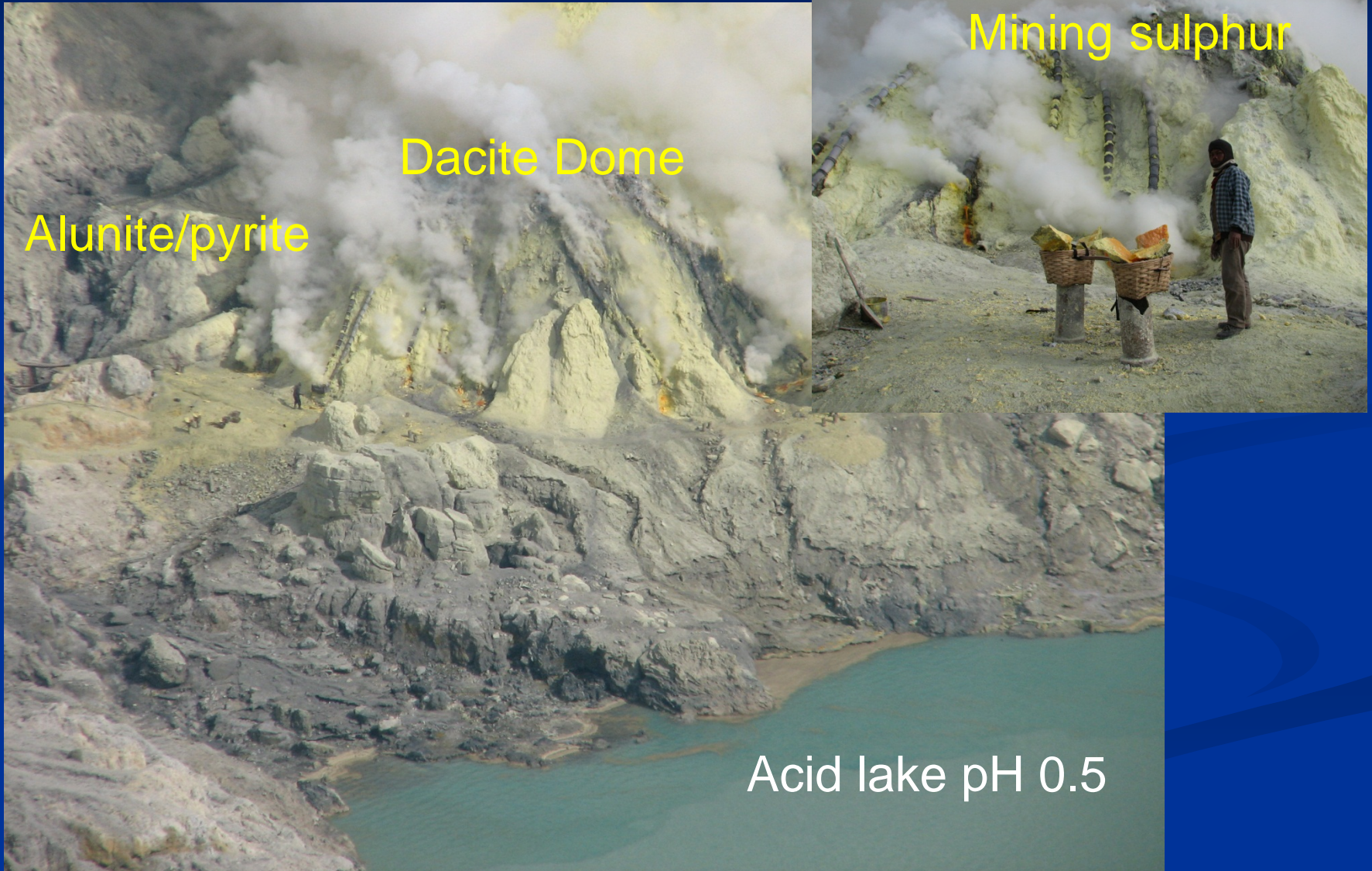
A possible explanation for “invisible gold” in pyrite – electrostatic attraction of negatively charged nanogold particles to the surfaces of positively charged pyrite

Williams-Jones et al. 2009

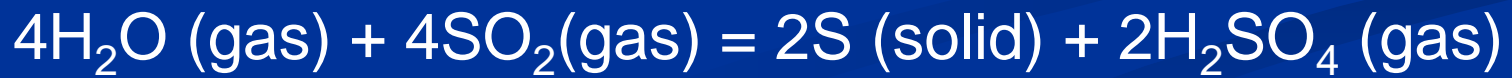
The Sangihe Model



Kawah Ijen - High Sulphidation Epithermal Deposit in the Making?



Sulphur condensation and acidity creation



Sampling the gases



Vapour-induced acid-sulphate Alteration



Acid-Sulphate Alteration

Pyroclastic rocks altered to alunite
($\text{KAl}_3(\text{SO}_4)_2(\text{OH})_6$) and pyrite

Leached andesite pillow containing
> 85 wt.% SiO_2 – residual silica



Acid Sulphate Alteration at Kawah Ijen

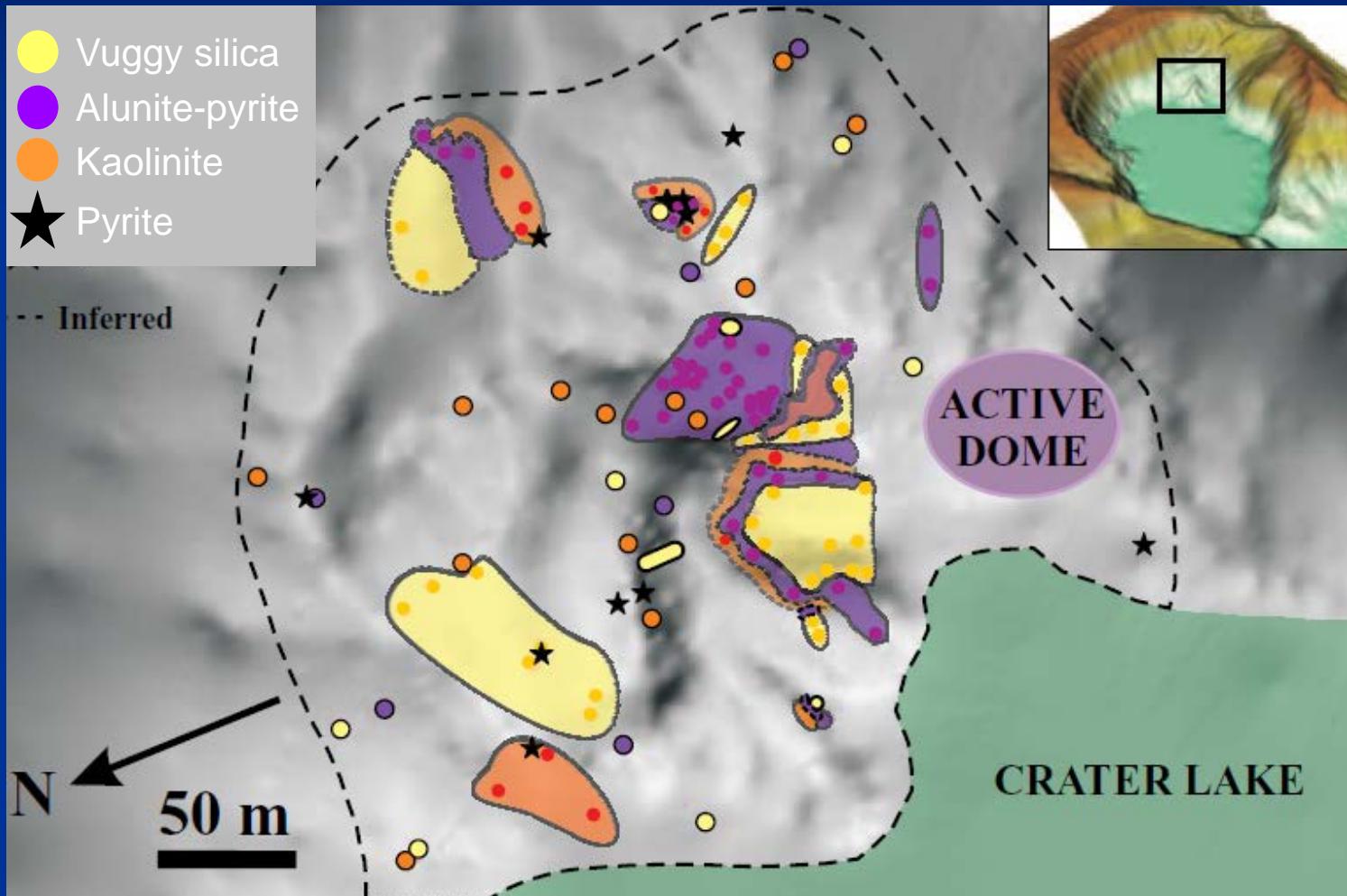
Alunite-pyrite alteration



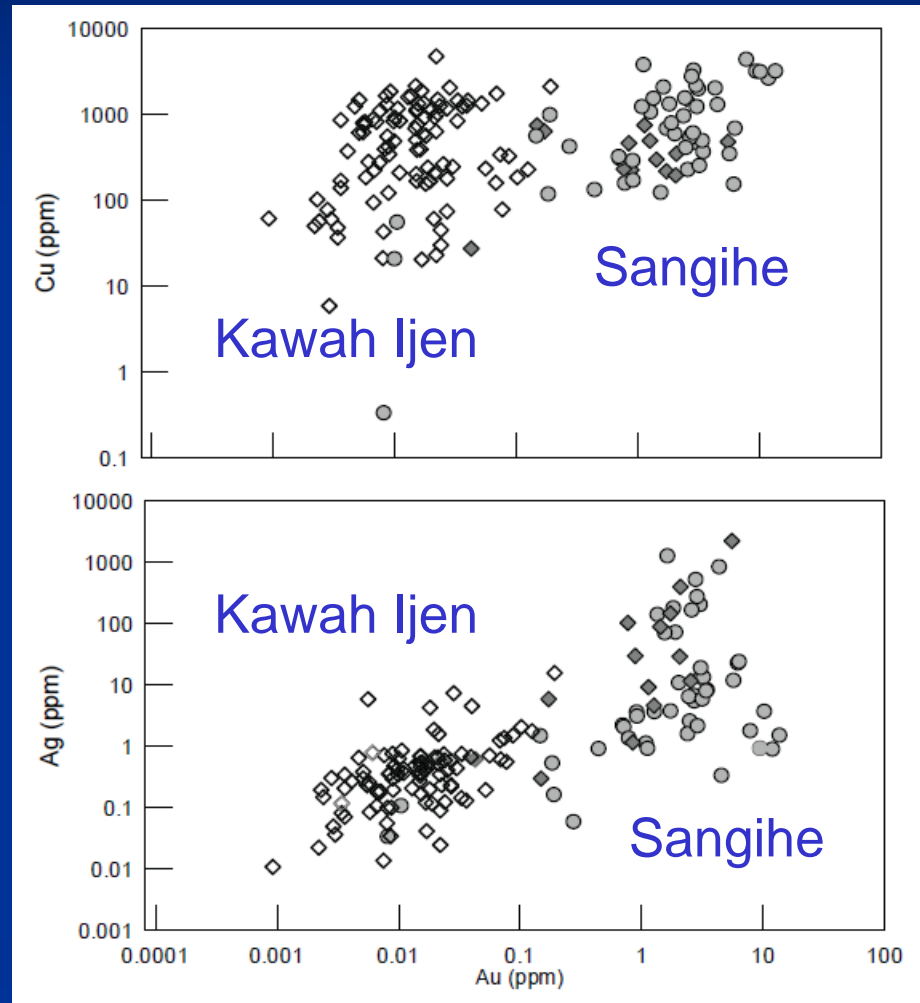
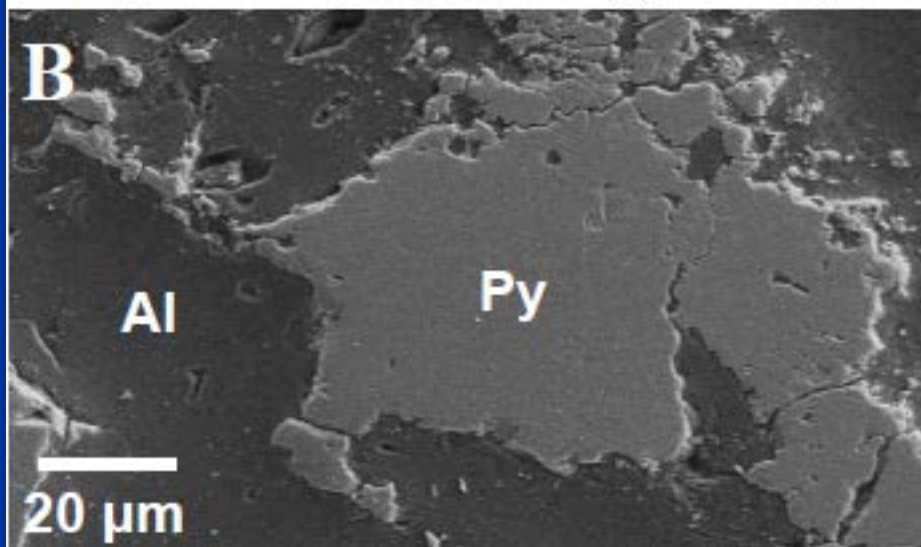
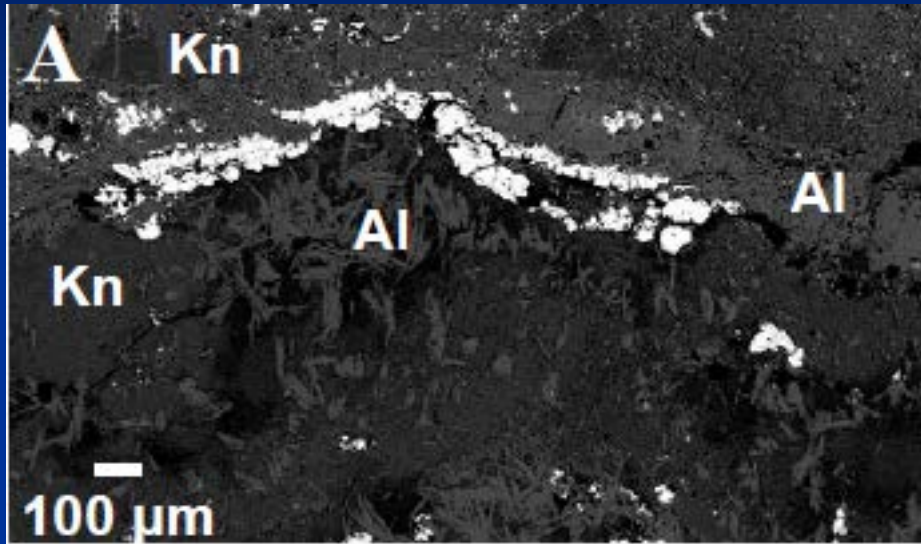
Alunite-pyrite vein



Distribution of Alteration at Kawah Ijen

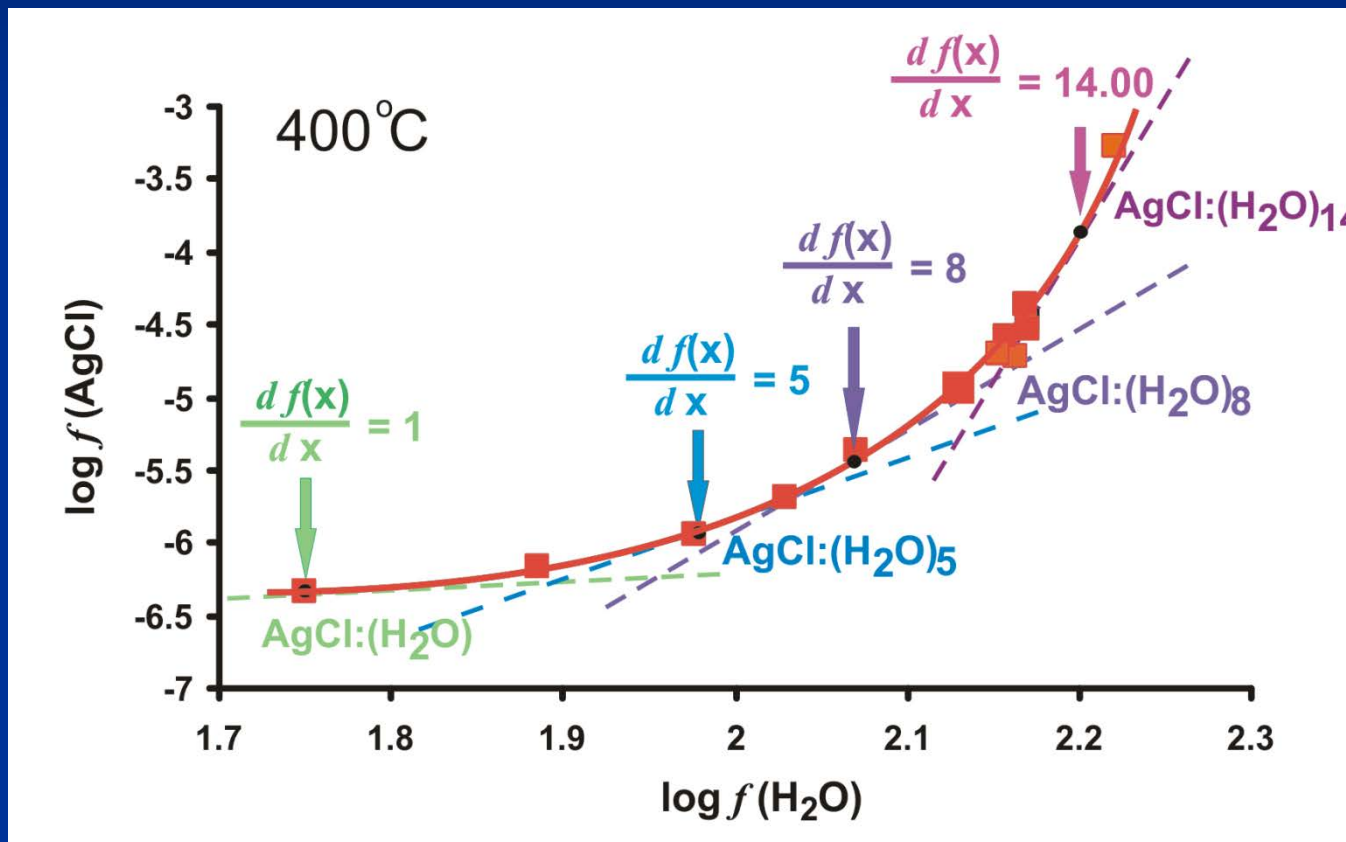


Gold Silver mineralisation at Kawah Ijen

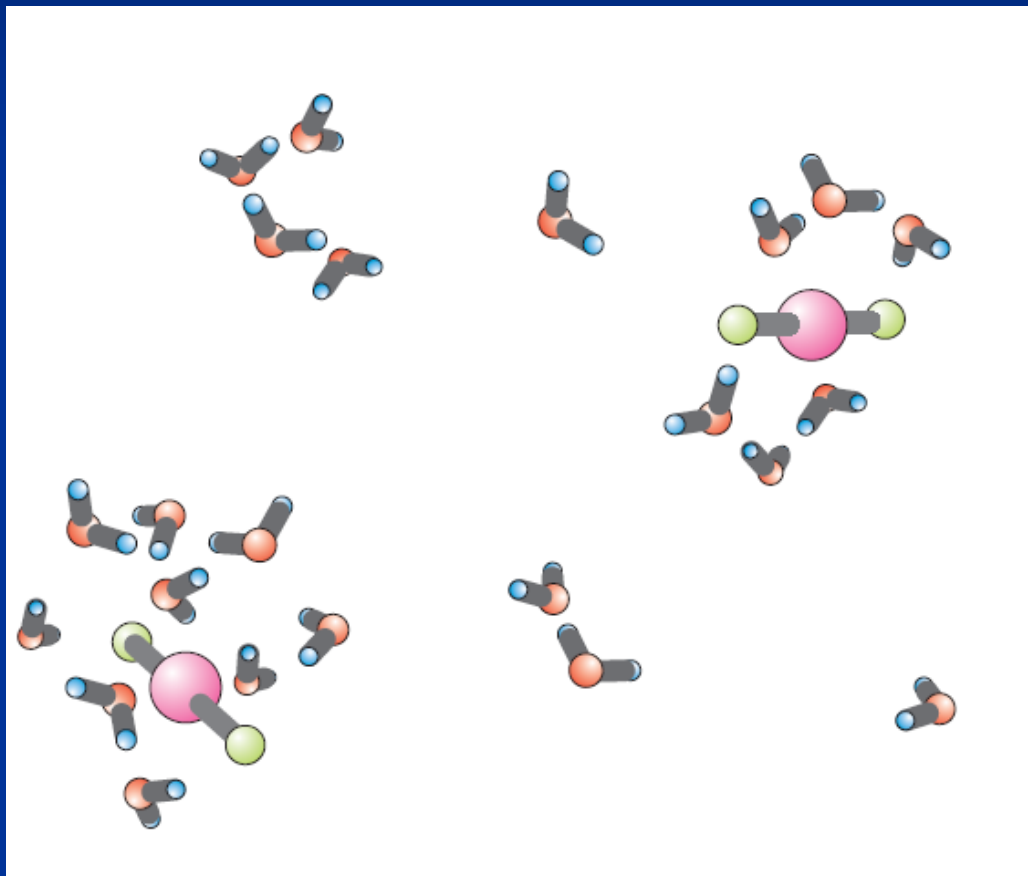


Solubility of Silver in HCl-H₂O Vapour

Silver solubility increases with hydration



Water Clusters Hydrating a Metal Species in the Gas Phase

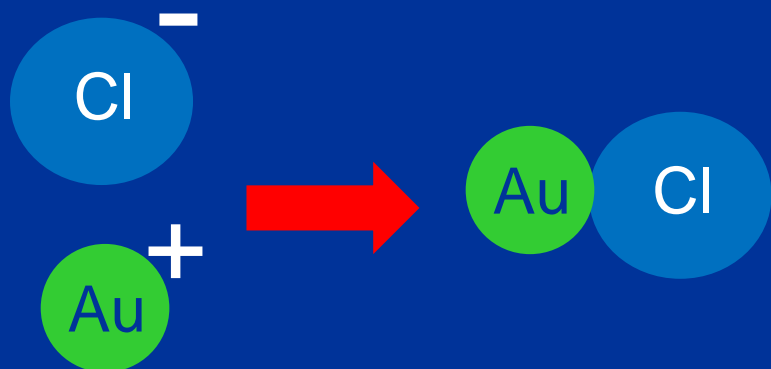


Williams-Jones and Migdisov (2014)

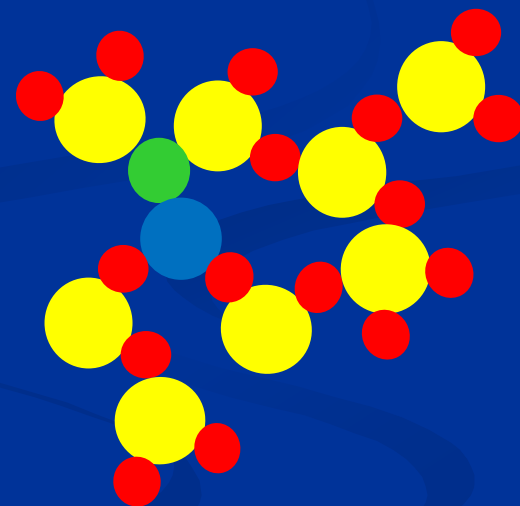
Think about clowns and balloons

The effects of complexation and particularly solvation by H₂O clusters make heavy metals volatile

Reaction

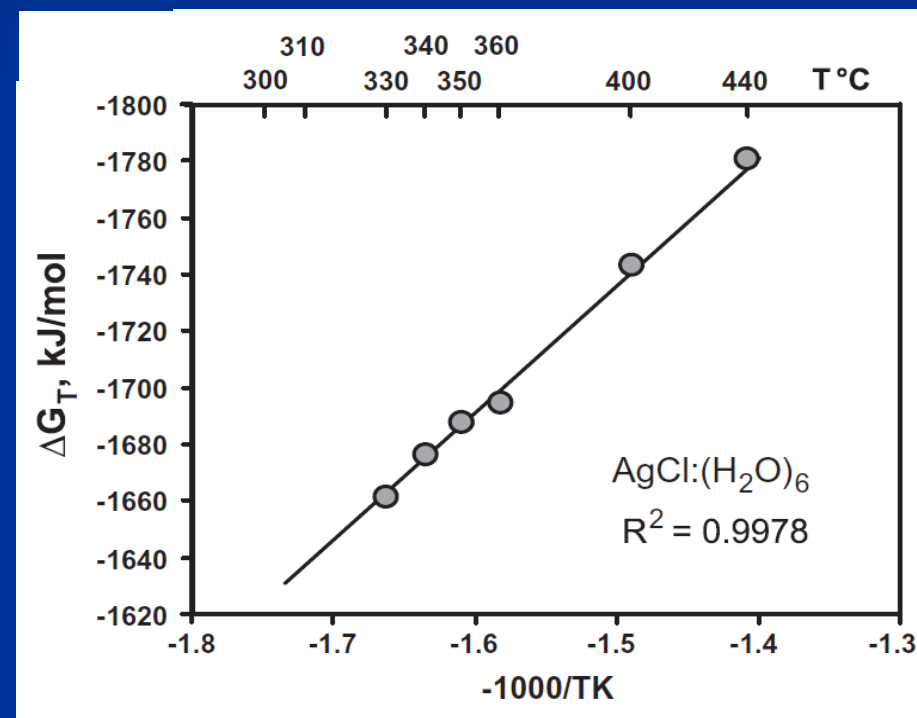
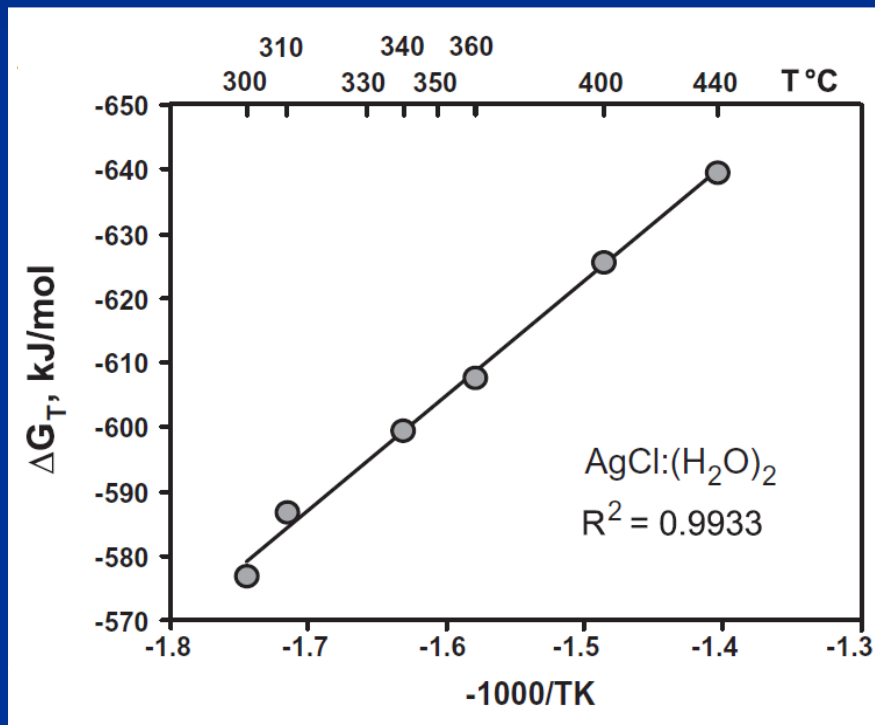


Hydration



Extracting Thermodynamic Data

The linear relationship between ΔG and reciprocal temperature enables extrapolation to high temperature

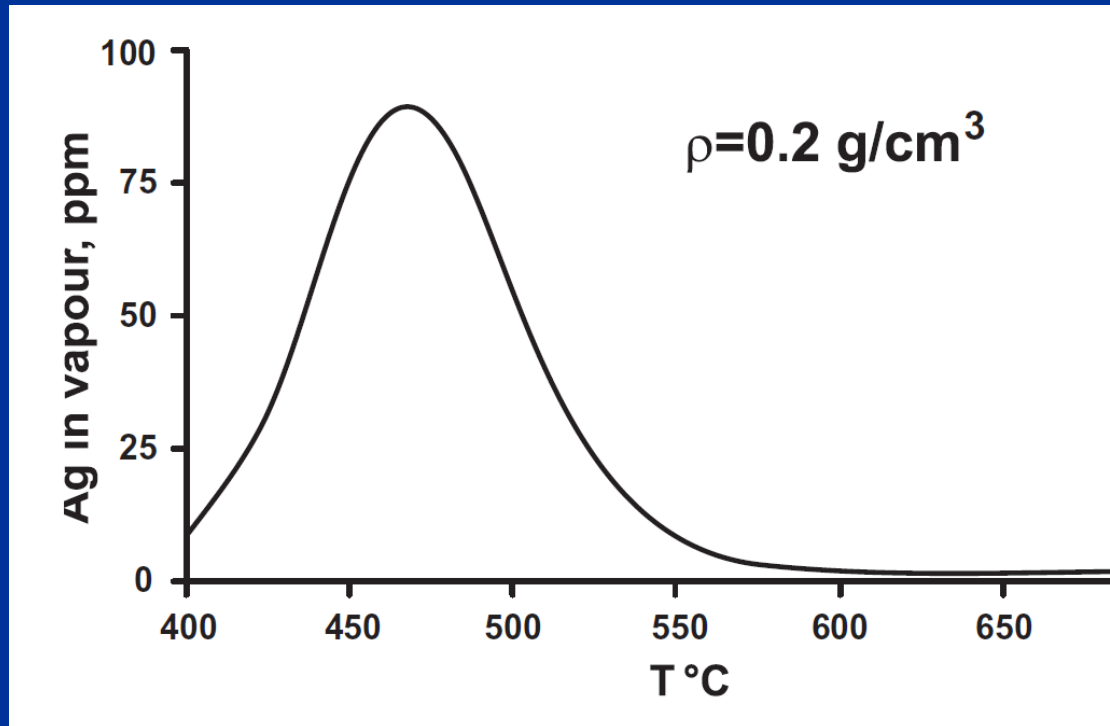


$$\text{Log } K = -\Delta G/RT$$

Solubility of Silver in HCl-H₂O Vapour

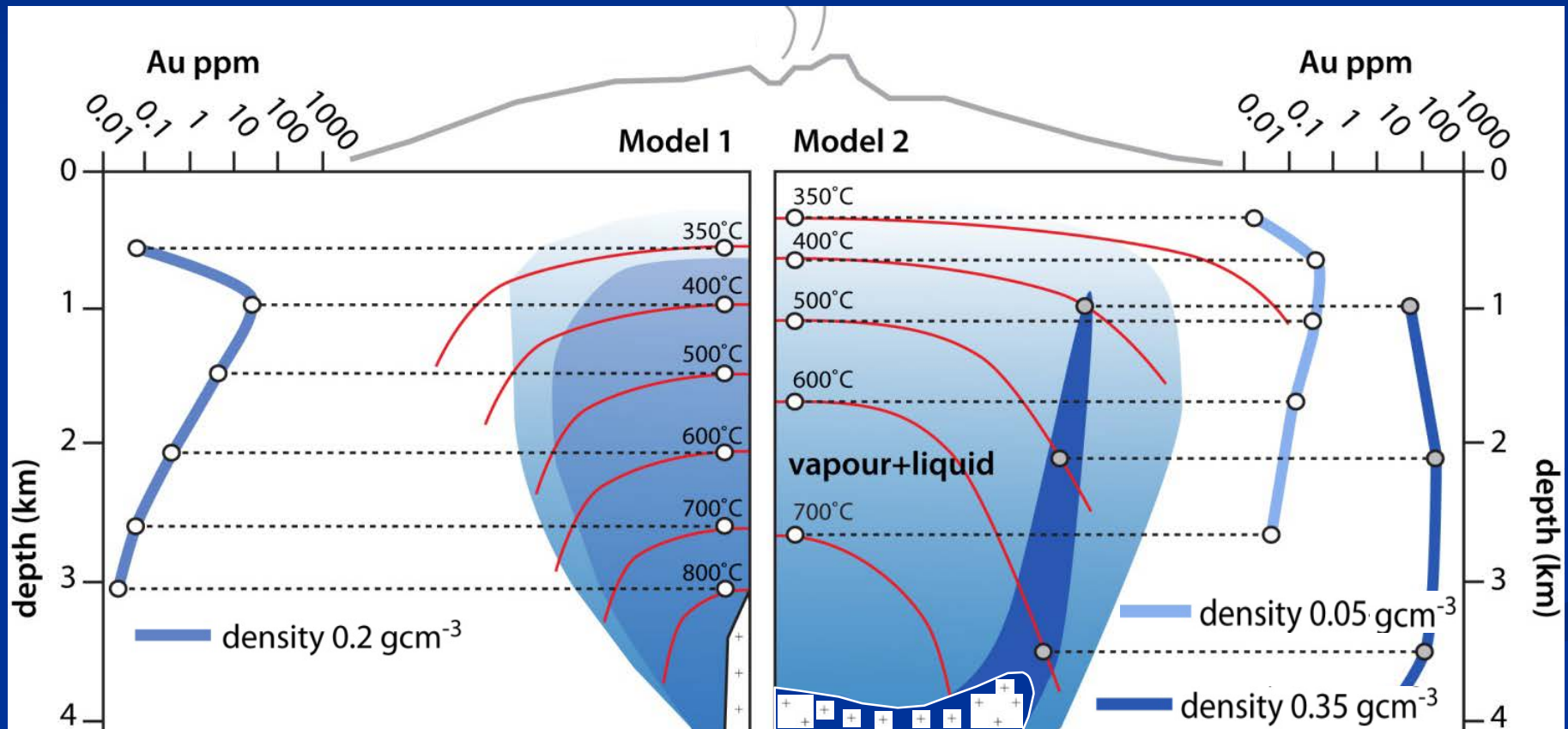
Hydration increases with increasing H₂O pressure or density but decreases with increasing temperature

Solubility increases with increasing temperature but reaches a maximum because of the effect of decreasing hydration



Epithermal Au Ore Formation

Vapour-dominated hydrothermal plume rises from magma transporting Au and depositing it as temperature drops below 400°C



References

- Chouinard, A., Williams-Jones, A.E., Leonardson, R.W., Hodgson, C.J., Silva, P., Téllez, C, Vega, J., and Rojas, F., 2005a, Geology and genesis of the multistage high-sulfidation epithermal Pascua Au-Ag-Cu deposit, Chile and Argentina: *Econ. Geol.*, v. 100, p. 463–490.
- Clark, J.R. and Williams-Jones, A.E., (1990) Analogues of epithermal gold-silver deposition in geothermal well scales: *Nature*, v. 346, no. 6285, pp 644-645.
- Cooke, D.R, Simmons, S.F., 2000. Characteristics and genesis of epithermal gold deposits. In: Hagemann, S.G., Brown, P.E. (Eds.), *Gold in 2000, Reviews in Econ. Geol.* vol. 13. Society of Economic Geology, Boulder, CO, pp. 221–244.
- Williams-Jones, A.E. and Heinrich, C.H., 2005, Vapor transport of metals and the formation of magmatic-hydrothermal ore deposits: *Econ. Geol.*, 100, p.1287-1312.
- King, J., Williams-Jones, A.E., van Hinsberg, V., and Williams-Jones, G. High sulfidation epithermal pyriote-hosted Au (Ag-Cu) ore formation by condensed magmatic vapors on Sangihe Island, Indonesia: *Economic Geology*, v. 109, p. 1705-1733.

- Scher, S., Williams-Jones, A.E., and Williams-Jones, G., 2013. Fumarolic activity, acid sulfate alteration and high sulfidation epithermal precious metal mineralization in the crater of Kawah Ijen volcano (Java, Indonesia). *Economic Geology*, 108, 1099-1118.
- Migdisov, A.A. and Williams-Jones, A.E., 2013. A predictive model for the transport of silver chloride by aqueous vapor in ore-forming magmatic-hydrothermal systems. *Geochimica et Cosmochimica Acta*, 104, 123-135.
- Hurting, N., and Williams-Jones, A.E., 2014. An experimental study of the transport of gold through hydration of AuCl in aqueous vapor and vapor-like fluids. *Geochimica et Cosmochimica Acta*, 127, 305-325.
- Williams-Jones, A.E., and Migdisov, A.A., 2014. Experimental constraints on the transport and deposition of metals in ore-forming hydrothermal systems. *Society of Economic Geologists, Special Publication 18*, 77-95.